Chapter 1 Fundamentals of Radiation for Atmospheric Applications

This text is intended for the study, understanding, and quantitative analysis of atmospheric radiation, a field in which the interactions of solar and terrestrial radiation with molecules, aerosols, and cloud particles in planetary atmospheres, as well as with the surface, are studied through the theory of radiative transfer and radiometric observations made from the ground, the air, and space. The field is closely associated with the investigation of atmospheric greenhouse effects resulting from external radiative perturbations in climate systems and the development of methodologies for inferring atmospheric and surface parameters by means of remote sensing. In the following, we begin with a discussion of various concepts, definitions, and units that are pertinent to the field of atmospheric radiation.

1.1 Concepts, Definitions, and Units

1.1.1 Electromagnetic Spectrum

The most important process responsible for energy transfer in the atmosphere is electromagnetic radiation. Electromagnetic radiation travels in wave form, and all electromagnetic waves travel at the same speed, the speed of light. This is $2.99793 \pm 1 \times 10^8$ m sec^{-1} in a vacuum and very nearly the same speed in air. Visible light, gamma rays, x-rays, ultraviolet light, infrared radiation, microwaves, television signals, and radio waves constitute the *electromagnetic spectrum*.

The retina of the human eye is sensitive to electromagnetic waves with frequencies between 4.3×10^{14} vibrations per second (usually written as cycles per second and abbreviated cps) and 7.5×10^{14} cps. Hence, this band of frequencies is called the *visible* region of the electromagnetic spectrum. The eye, however, does not respond to frequencies of electromagnetic waves higher than 7.5×10^{14} cps. Such waves, lying beyond the violet edge of the spectrum, are called *ultraviolet* light. The human eye also does not respond to electromagnetic waves with frequencies lower than 4.3×10^{14} cps. These waves, having frequencies lower than the lowest frequency of visible light at the red end of the spectrum and higher than about 3×10^{12} cps, are called *infrared light* or *infrared radiation*. Just beyond the infrared portion of the

spectrum are *microwaves,* which cover the frequencies from about 3×10^{10} cps to 3×10^{12} cps. The most significant spectral regions associated with radiative energy transfer in planetary atmospheres lie between ultraviolet light and microwaves.

The *x-ray* region of the electromagnetic spectrum consists of waves with frequencies ranging from about 3×10^{16} cps to 3×10^{18} cps, and is adjacent to the ultraviolet region in the spectrum. The *gamma-ray* region of the spectrum has the highest frequencies of all, ranging upward from about 3×10^{19} cps. *Radio* waves have the lowest frequencies in the spectrum, extending downward from about 3×10^{5} cps.

Electromagnetic waves are often described in terms of their wavelength rather than their frequency. The following general formula connects frequency $\tilde{\nu}$ and wavelength λ:

$$\lambda = c/\tilde{\nu}, \tag{1.1.1}$$

where c represents the speed of light in a vacuum. It is conventional to use micrometers (μm; 1 μm $= 10^{-4}$ cm) to denote the wavelengths of radiation from the sun. Other units, known as nanometers (nm; 1 nm $= 10^{-7}$ cm $= 10^{-3}$ μm) and angstroms (Å; 1 Å $= 10^{-4}$ μm), have also been frequently used, particularly for ultraviolet radiation. Equation (1.1.1) is valid for any type of wave and is not restricted to electromagnetic waves. It is customary to use wavenumber ν to describe the characteristics of infrared radiation. It is defined by

$$\nu = \tilde{\nu}/c = 1/\lambda. \tag{1.1.2}$$

Thus, a 10 micrometer (μm) wavelength is equal to a 1000 cm^{-1} wavenumber. In the microwave region, however, a frequency unit called gigahertz (GHz) is commonly used. One GHz is equal to 10^{9} cycles per second. It follows that 1 cm is equivalent to 30 GHz. Figure 1.1 shows the complete electromagnetic spectrum along with each region's corresponding frequency, wavenumber, and wavelength.

1.1.2 Solid Angle

The analysis of a radiation field often requires the consideration of the amount of radiant energy confined to an element of solid angle. A solid angle is defined as the ratio of the area σ of a spherical surface intercepted at the core to the square of the radius, r, as indicated in Fig. 1.2. It can be written as

$$\Omega = \sigma/r^2. \tag{1.1.3}$$

Units of solid angle are expressed in terms of the steradian (sr). For a sphere whose surface area is $4\pi r^2$, its solid angle is 4π sr.

To obtain a differential elemental solid angle, we construct a sphere whose central point is denoted as O. Assuming a line through point O moving in space and intersecting an arbitrary surface located at a distance r from point O, then as is evident from Fig. 1.3, the differential area in polar coordinates is given by

$$d\sigma = (r\,d\theta)(r \sin\theta\, d\phi). \tag{1.1.4}$$

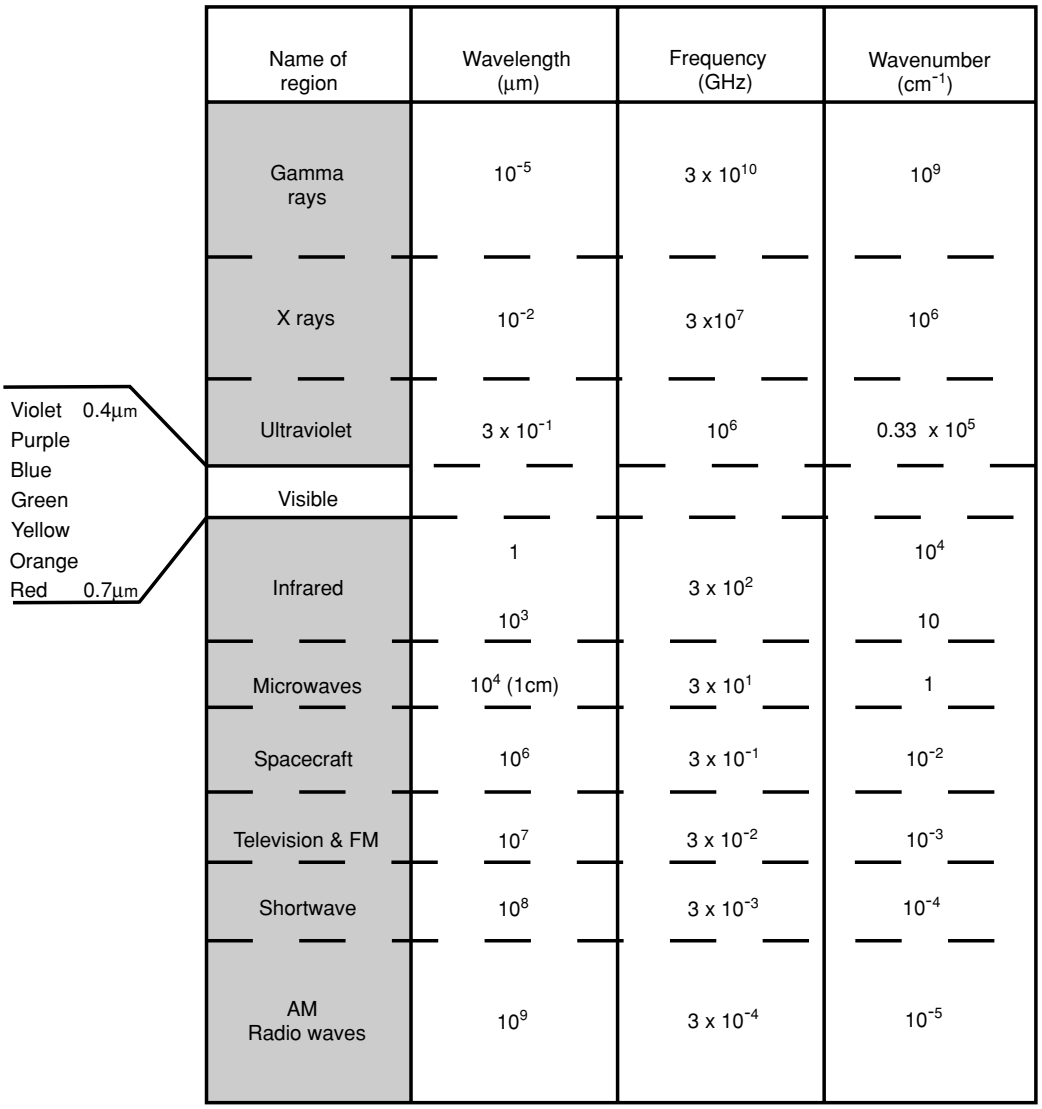

Figure 1.1 The electromagnetic spectrum in terms of wavelength in μm, frequency in GHz, and wavenumber in cm^{-1}.

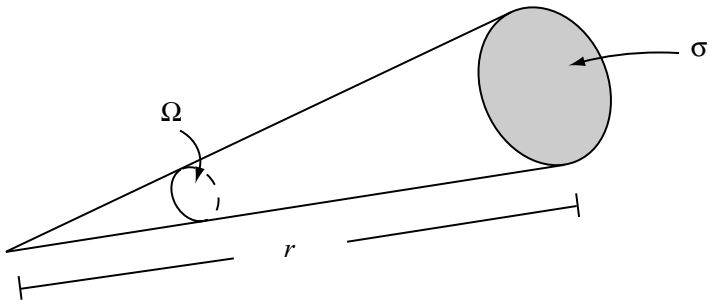

Figure 1.2 Definition of a solid angle Ω, where σ denotes the area and r is the distance.

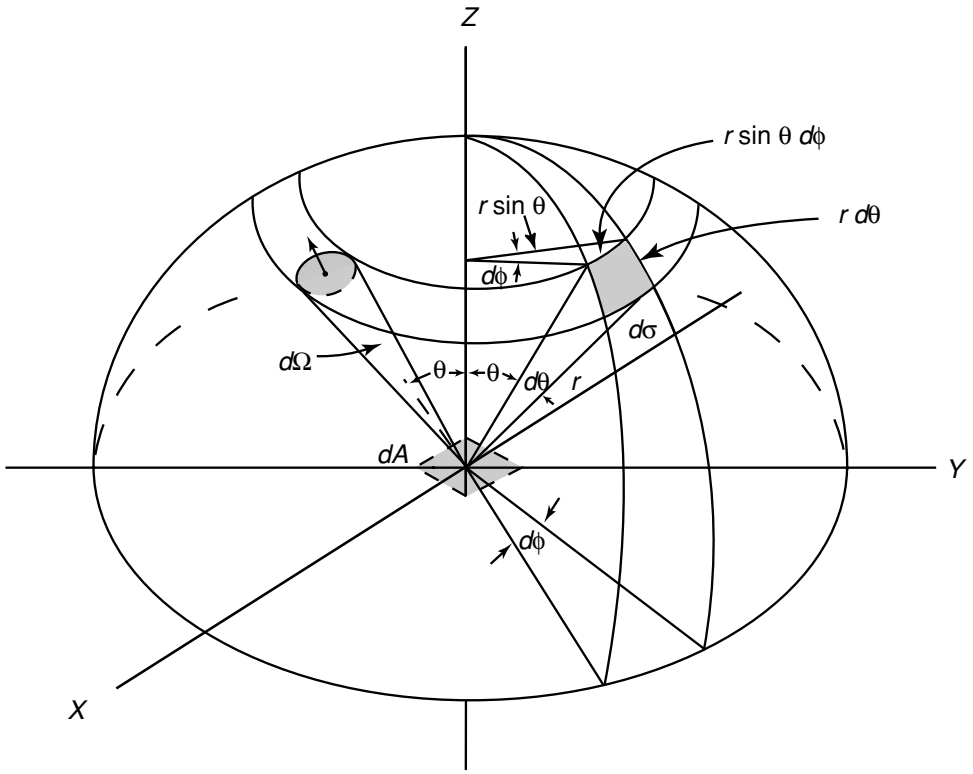

Figure 1.3 Illustration of a differential solid angle and its representation in polar coordinates. Also shown for demonstrative purposes is a pencil of radiation through an element of area dA in directions confined to an element of solid angle $d\Omega$. Other notations are defined in the text.

Hence, the differential solid angle is

$$d\Omega = d\sigma/r^2 = \sin\theta\, d\theta\, d\phi, \tag{1.1.5}$$

where θ and ϕ denote the zenith and azimuthal angles, respectively, in polar coordinates.

1.1.3 Basic Radiometric Quantities

Consider the differential amount of radiant energy dE_λ in a time interval dt and in a specified wavelength interval, λ to $\lambda + d\lambda$, which crosses an element of area dA depicted in Fig. 1.3, in directions confined to a differential solid angle, which is oriented at an angle θ to the normal of dA. This energy is expressed in terms of the specific intensity I_λ by

$$dE_\lambda = I_\lambda \cos\theta\, dA\, d\Omega\, d\lambda\, dt, \tag{1.1.6}$$

where $\cos\theta\, dA$ denotes the effective area at which the energy is being intercepted. Equation (1.1.6) defines the *monochromatic intensity* (or *radiance*) in a general way as follows:

$$I_\lambda = \frac{dE_\lambda}{\cos\theta\, d\Omega\, d\lambda\, dt\, dA}. \tag{1.1.7}$$

Thus, the intensity is in units of energy per area per time per wavelength and per steradian. It is evident that the intensity implies a directionality in the radiation stream. Commonly, the intensity is said to be confined in a pencil of radiation.

The *monochromatic flux density* or the *monochromatic irradiance* of radiant energy is defined by the normal component of I_λ integrated over the entire hemispheric solid angle and may be written as

$$F_\lambda = \int_\Omega I_\lambda \cos\theta \, d\Omega. \tag{1.1.8}$$

In polar coordinates, we write

$$F_\lambda = \int_0^{2\pi} \int_0^{\pi/2} I_\lambda (\theta, \phi) \cos\theta \, \sin\theta \, d\theta \, d\phi. \tag{1.1.9}$$

For isotropic radiation (i.e., if the intensity is independent of the direction), the monochromatic flux density is then

$$F_\lambda = \pi I_\lambda. \tag{1.1.10}$$

The total flux density of radiant energy, or irradiance, for all wavelengths (energy per area per time), can be obtained by integrating the monochromatic flux density over the entire electromagnetic spectrum:

$$F = \int_0^\infty F_\lambda \, d\lambda. \tag{1.1.11}$$

Moreover, the total flux f, or radiant power W (energy per time), is defined by

$$f = \int_A F \, dA. \tag{1.1.12}$$

The monochromatic flux density in the frequency domain may be written in the form

$$F_{\tilde{\nu}} = \frac{dF}{d\tilde{\nu}}. \tag{1.1.13}$$

From the relationship between wavelength and frequency denoted in Eq. (1.1.1), we have

$$F_{\tilde{\nu}} = -(\lambda^2/c) F_\lambda. \tag{1.1.14}$$

Likewise, the intensity in wavelength and frequency domains is connected by

$$I_{\tilde{\nu}} = -(\lambda^2/c) I_\lambda. \tag{1.1.15}$$

A similar relation between the monochromatic flux density, or intensity, in wavenumber and wavelength (or frequency) domains may be expressed by means of Eq. (1.1.2).

When the flux density or the irradiance is from an emitting surface, the quantity is called the *emittance*. When expressed in terms of wavelength, it is referred to as the *monochromatic emittance*. The intensity or the radiance is also called the *brightness* or *luminance* (photometric brightness). The total flux from an emitting surface is

Table 1.1
Symbols, Dimensions, and Units of Various Radiometric Quantities

Symbol	Quantity	Dimension[a]	Unit[b]
E	Energy	ML^2T^{-2}	Joule (J)
f	Flux (luminosity)	ML^2T^{-3}	Joule per second (J sec^{-1}, W)
F	Flux density (irradiance) Emittance	MT^{-3}	Joule per second per square meter (W m^{-2})
I	Intensity (radiance) Brightness (luminance)	MT^{-3}	Joule per second per square meter per steradian ($\text{W m}^{-2}\ \text{sr}^{-1}$)

[a] M is mass, L is length, and T is time.
[b] 1 watt (W) = 1 J sec^{-1}.

often called *luminosity*. The basic radiometric quantities are summarized in Table 1.1, along with their symbols, dimensions, and units.

1.1.4 Concepts of Scattering and Absorption

Most of the light that reaches our eyes comes not directly from its source but indirectly through the process of *scattering*. We see diffusely scattered sunlight when we look at clouds or at the sky. Land and water surfaces and the objects surrounding us are visible through the light that they scatter. An electric lamp does not send us light directly from the luminous filament but usually glows with the light that has been scattered by the glass bulb. Unless we look directly at a light source, such as the sun, a flame, or an incandescent filament with a clear bulb, we see light that has been scattered. In the atmosphere, we see many colorful examples of scattering generated by molecules, aerosols, and clouds containing water droplets and ice crystals. Blue sky, white clouds, and magnificent rainbows and halos, to name a few, are all optical phenomena produced by scattering. Scattering is a fundamental physical process associated with light and its interaction with matter. It occurs at all wavelengths throughout the entire electromagnetic spectrum.

Scattering is a physical process by which a particle in the path of an electromagnetic wave continuously abstracts energy from the incident wave and reradiates that energy in all directions. Therefore, the particle may be thought of as a point source of the scattered energy. In the atmosphere, the particles responsible for scattering range in size from gas molecules ($\sim 10^{-4}$ μm) to aerosols (~ 1 μm), water droplets (~ 10 μm), ice crystals (~ 100 μm), and large raindrops and hail particles (~ 1 cm). The effect of particle size on scattering is inferred by a physical term called the *size parameter*. For a spherical particle, it is defined as the ratio of the particle circumference to the incident wavelength, λ; i.e., $x = 2\pi a/\lambda$, where a is the particle radius. If $x \ll 1$, the scattering is called *Rayleigh scattering*. An excellent example of this case is the scattering of visible light (0.4–0.7 μm) by atmospheric molecules, leading to the explanation of blue sky and sky polarization to be discussed in Chapter 3. For

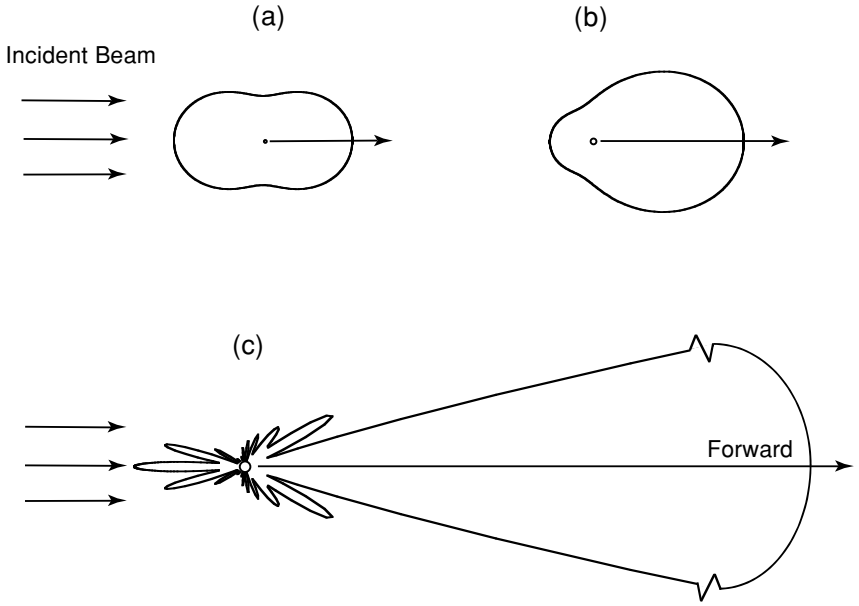

Figure 1.4 Demonstrative angular patterns of the scattered intensity from spherical aerosols of three sizes illuminated by the visible light of 0.5 μm: (a) 10^{-4} μm, (b) 0.1 μm, and (c) 1 μm. The forward scattering pattern for the 1 μm aerosol is extremely large and is scaled for presentation purposes.

particles whose sizes are comparable to or larger than the wavelength, i.e., $x \gtrsim 1$, the scattering is customarily referred to as *Lorenz–Mie scattering*. The mathematical theory of Lorenz–Mie scattering for spherical particles will be presented in Chapter 5. Figure 1.4 illustrates the scattering patterns of spherical aerosols of size 10^{-4}, 0.1, and 1 μm illuminated by a visible light of 0.5 μm. A small particle tends to scatter light equally in the forward and backward directions. When the particle becomes larger, the scattered energy becomes increasingly concentrated in the forward direction with increasingly complex scattering features. Because of the spherical symmetry with respect to the incoming light beam, the scattering patterns for other planes are the same as the ones presented in Fig. 1.4. The scattering of sunlight by spherical cloud droplets and raindrops produces the magnificent rainbows and glory that we see in our daily life.

In situ observations and electronic microscopic photography have shown that aerosols in the atmosphere, such as minerals, soot, and even oceanic particles, exhibit a wide variety of shapes ranging from quasi-spherical to highly irregular geometric figures with internal structure. The shape and size of ice crystals are governed by temperature and supersaturation, but they generally have a basic hexagonal structure. In the atmosphere, if ice crystal growth involves collision and coalescence, the crystal's shape can be extremely complex. Recent observations based on aircraft optical probes and replicator techniques for widespread midlatitude, tropical, arctic, and contrail cirrus show that these clouds are largely composed of ice crystals in the shape of bullet rosettes, solid and hollow columns, plates, and aggregates, and ice crystals with irregular surfaces with sizes ranging from a few micrometers to thousands of micrometers. The scattering of sunlight by some of the defined ice crystals produces

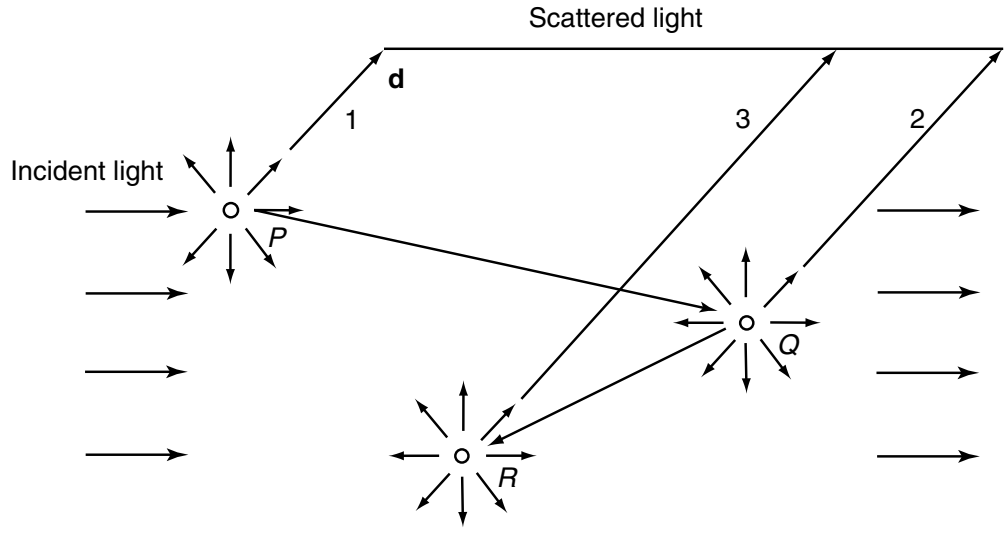

Figure 1.5 Multiple scattering process involving first (P), second (Q), and third (R) order scattering in the direction denoted by **d.**

fascinating optical phenomena including 22° and 46° halos, sundogs, and numerous arcs and bright spots. Light scattering by nonspherical and inhomogeneous particles, a contemporary research subject, will be covered in Chapter 5, which presents a combination of geometric ray-tracing and numerical solution approaches.

In atmospheric scattering, it is generally assumed that the light scattered by molecules and particulates has the same frequency (or wavelength) as the incident light. It is noted, however, that high-energy laser light can produce phenomena such as Raman scattering in shift frequencies, which can be employed for the remote sensing of water vapor. Atmospheric molecules and particulates are separated widely enough so that each particle scatters light in exactly the same way as if all other particles did not exist. This is referred to as *independent scattering*. The assumption of independent scattering greatly simplifies the problem of light scattering by a collection of particles, because it allows the use of energy quantity instead of electric field in the analysis of the propagation of electromagnetic waves in planetary atmospheres.

In a scattering volume, which contains many particles, each particle is exposed to, and also scatters, the light that has already been scattered by other particles. To demonstrate this concept we refer to Fig. 1.5. A particle at position P removes the incident light by scattering just once, i.e., single scattering, in all directions. Meanwhile, a portion of this scattered light reaches the particle at position Q, where it is scattered again in all directions. This is called *secondary scattering*. Likewise, a subsequent third-order scattering involving the particle at position R takes place. Scattering more than once is called *multiple scattering*. It is apparent from Fig. 1.5 that some of the incident light that has been first scattered away from direction **d** may reappear in this direction by means of multiple scattering. Multiple scattering is an important process for the transfer of radiant energy in the atmosphere, especially when aerosols and clouds are involved. Chapter 6 deals with the theory of multiple scattering in planetary atmospheres.

Scattering is often accompanied by absorption. Grass looks green because it scatters green light while it absorbs red and blue light. The absorbed energy is converted into some other form, and it is no longer present as red or blue light. In molecular atmospheres, there is very little absorption of energy in the visible spectrum. Clouds also absorb very little visible light. Both scattering and absorption remove energy from a beam of light traversing the medium. The beam of light is attenuated, and we call this attenuation *extinction*. Thus, extinction is a result of scattering plus absorption. In a nonabsorbing medium, scattering is the sole process of extinction.

In the field of light scattering and radiative transfer, it is customary to use a term called *cross section,* analogous to the geometrical area of a particle, to denote the amount of energy removed from the original beam by the particle. When the cross section is associated with a particle dimension, its units are denoted in terms of area (cm^2). Thus, the extinction cross section, in units of area, is the sum of the scattering and absorption cross sections. However, when the cross section is in reference to unit mass, its units are given in area per mass ($cm^2\ g^{-1}$). In this case, the term mass extinction cross section is used in radiative transfer. The mass extinction cross section is, therefore, the sum of the mass absorption and mass scattering cross sections. Furthermore, when the extinction cross section is multiplied by the particle number density (cm^{-3}), or when the mass extinction cross section is multiplied by the density ($g\ cm^{-3}$), the quantity is referred to as the *extinction coefficient,* whose units are given in terms of length (cm^{-1}). In the field of infrared radiative transfer, the mass absorption cross section is simply referred to as the *absorption coefficient*.

The absorption of energy by particles and molecules leads to emission. The concept of emission is associated with blackbody radiation and will be discussed in the following section. In addition, a number of minor atmospheric constituents exhibit complicated absorption line structures in the infrared region. Section 1.3 and Chapter 4 will provide discussions of the fundamentals of line formation and the transfer of infrared radiation in the atmosphere. A fundamental understanding of the scattering and absorption processes in the atmosphere is imperative for the study of the radiation budget and climate of planetary atmospheres and for the exploration of remote sounding techniques to infer atmospheric composition and structure.

1.2 Blackbody Radiation Laws

The laws of blackbody radiation are basic to an understanding of the absorption and emission processes. A blackbody is a basic concept in physics and can be visualized by considering a cavity with a small entrance hole, as shown in Fig. 1.6. Most of the radiant flux entering this hole from the outside will be trapped within the cavity, regardless of the material and surface characteristics of the wall. Repeated internal reflections occur until all the fluxes are absorbed by the wall. The probability that any of the entering flux will escape back through the hole is so small that the interior appears dark. The term *blackbody* is used for a configuration of material where absorption is complete. Emission by a blackbody is the converse of absorption. The flux

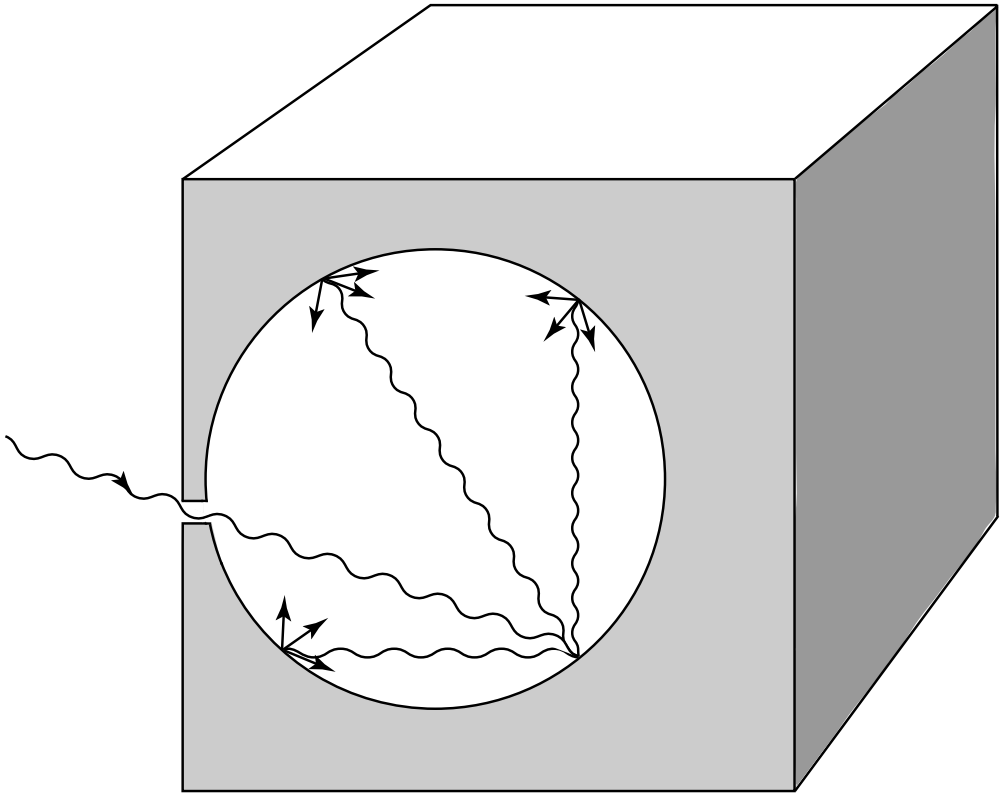

Figure 1.6 A blackbody radiation cavity to illustrate that absorption is complete.

emitted by any small area of the wall is repeatedly reflected and at each encounter with the wall, the flux is weakened by absorption and strengthened by new emission. After numerous encounters, emission and absorption reach an equilibrium condition with respect to the wall temperature. In the following, we present four fundamental laws that govern blackbody radiation, beginning with Planck's law.

1.2.1 Planck's Law

In his pursuit of a theoretical explanation for cavity radiation, Planck (1901) assumed that the atoms that make up the wall behave like tiny electromagnetic oscillators, each with a characteristic frequency of oscillation. The oscillators emit energy into the cavity and absorb energy from it. In his analysis, Planck was led to make two assumptions about the atomic oscillators. First, Planck postulated that an oscillator can only have energy given by

$$E = nh\tilde{\nu}, \tag{1.2.1}$$

where $\tilde{\nu}$ is the oscillator frequency, h is Planck's constant, and n is called the quantum number and can take on only integral values. Equation (1.2.1) asserts that the oscillator energy is quantized. Although later developments revealed that the correct formula for a harmonic oscillator is $E = (n + 1/2)h\tilde{\nu}$ [see Eq. (1.3.7)], the change introduces no difference to Planck's conclusions. Secondly, Planck postulated that the oscillators

do not radiate energy continuously, but only in jumps, or in quanta. These quanta of energy are emitted when an oscillator changes from one to another of its quantized energy states. Hence, if the quantum number changes by one unit, the amount of radiated energy is given by

$$\Delta E = \Delta n h\tilde{\nu} = h\tilde{\nu}. \tag{1.2.2}$$

Determination of the emitted energy requires knowing the total number of oscillators with frequency $\tilde{\nu}$ for all possible states in accord with Boltzmann statistics, as presented in Appendix A. Following the two preceding postulations and normalization of the average emitted energy per oscillator, the Planck function in units of energy/area/time/sr/frequency is given by

$$B_{\tilde{\nu}}(T) = \frac{2h\tilde{\nu}^3}{c^2(e^{h\tilde{\nu}/KT} - 1)}, \tag{1.2.3}$$

where K is Boltzmann's constant, c is the velocity of light, and T is the absolute temperature. The Planck and Boltzmann constants have been determined through experimentation and are $h = 6.626 \times 10^{-34}$ J sec and $K = 1.3806 \times 10^{-23}$ J deg^{-1}.

The Planck function relates the emitted monochromatic intensity to the frequency and the temperature of the emitting substance. By utilizing the relation between frequency and wavelength shown in Eq. (1.1.15), Eq. (1.2.3) can be rewritten as follows:

$$B_\lambda(T) = \frac{2hc^2}{\lambda^5(e^{hc/K\lambda T} - 1)} = \frac{C_1\lambda^{-5}}{\pi(e^{C_2/\lambda T} - 1)}, \tag{1.2.4}$$

where $C_1 = 2\pi hc^2$ and $C_2 = hc/K$ are known as the first and second radiation constants, respectively. Figure 1.7 shows curves of $B_\lambda(T)$ versus wavelength for a number of emitting temperatures. It is evident that the blackbody radiant intensity increases with temperature and that the wavelength of the maximum intensity decreases with increasing temperature. The Planck function behaves very differently when $\lambda \to \infty$, referred to as the *Rayleigh–Jeans distribution,* and when $\lambda \to 0$, referred to as the *Wien distribution*.

1.2.2 Stefan–Boltzmann Law

The total radiant intensity of a blackbody can be derived by integrating the Planck function over the entire wavelength domain from 0 to ∞. Hence,

$$B(T) = \int_0^\infty B_\lambda(T)\, d\lambda = \int_0^\infty \frac{2hc^2\lambda^{-5}}{(e^{hc/K\lambda T} - 1)}\, d\lambda. \tag{1.2.5}$$

On introducing a new variable $x = hc/k\lambda T$, Eq. (1.2.5) becomes

$$B(T) = \frac{2k^4T^4}{h^3c^2}\int_0^\infty \frac{x^3 dx}{(e^x - 1)}. \tag{1.2.6}$$

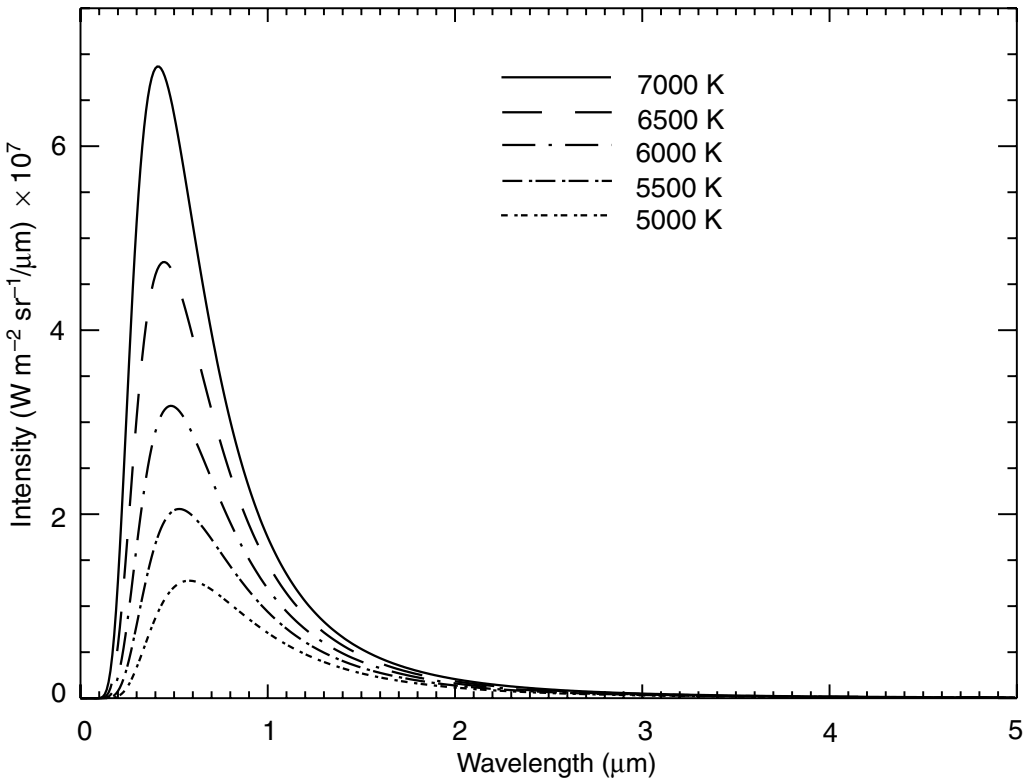

Figure 1.7 Blackbody intensity (Planck function) as a function of wavelength for a number of emitting temperatures.

The integral term in Eq. (1.2.6) is equal to $\pi^4/15$. Thus, defining

$$b = 2\pi^4 K^4/(15c^2h^3), \tag{1.2.7}$$

we then have

$$B(T) = bT^4. \tag{1.2.8}$$

Since blackbody radiation is isotropic, the flux density emitted by a blackbody is therefore [see Eq. (1.1.10)]

$$F = \pi B(T) = \sigma T^4, \tag{1.2.9}$$

where σ is the Stefan–Boltzmann constant and is equal to 5.67×10^{-8} J m^{-2} sec^{-1} deg^{-4}. Equation (1.2.9) states that the flux density emitted by a blackbody is proportional to the fourth power of the *absolute* temperature. This is the Stefan–Boltzmann law, fundamental to the analysis of broadband infrared radiative transfer.

1.2.3 Wien's Displacement Law

Wien's displacement law states that the wavelength of the maximum intensity of blackbody radiation is inversely proportional to the temperature. By differentiating

the Planck function with respect to wavelength, and by setting the result equal to zero, i.e.,

$$\frac{\partial B_\lambda(T)}{\partial \lambda} = 0, \tag{1.2.10}$$

we obtain the wavelength of the maximum (Exercise 1.4)

$$\lambda_m = a/T, \tag{1.2.11}$$

where $a = 2.897 \times 10^{-3}$ m deg. From this relationship, we can determine the temperature of a blackbody from the measurement of the maximum monochromatic intensity. The dependence of the position of the maximum intensity on temperature is evident from the blackbody curves displayed in Fig. 1.7.

1.2.4 Kirchhoff's Law

The preceding three fundamental laws are concerned with the radiant intensity emitted by a blackbody, which is dependent on the emitting wavelength and the temperature of the medium. A medium may absorb radiation of a particular wavelength, and at the same time also emit radiation of the same wavelength. The rate at which emission takes place is a function of temperature and wavelength. This is the fundamental property of a medium under the condition of *thermodynamic equilibrium*. The physical statement regarding absorption and emission was first proposed by Kirchhoff (1860).

To understand the physical meaning of Kirchhoff's law, we consider a perfectly insulated enclosure having black walls. Assume that this system has reached the state of thermodynamic equilibrium characterized by uniform temperature and isotropic radiation. Because the walls are black, radiation emitted by the system to the walls is absorbed. Moreover, because there is an equilibrium, the same amount of radiation absorbed by the walls is also emitted. Since the blackbody absorbs the maximum possible radiation, it has to emit that same amount of radiation. If it emitted more, equilibrium would not be possible, and this would violate the second law of thermodynamics. Radiation within the system is referred to as blackbody radiation as noted earlier, and the amount of radiant intensity is a function of temperature and wavelength.

On the basis of the preceding discussion, the emissivity of a given wavelength, ε_λ (defined as the ratio of the emitting intensity to the Planck function), of a medium is equal to the absorptivity, A_λ (defined as the ratio of the absorbed intensity to the Planck function), of that medium under thermodynamic equilibrium. Hence, we may write

$$\varepsilon_\lambda = A_\lambda. \tag{1.2.12}$$

A medium with an absorptivity A_λ absorbs only A_λ times the blackbody radiant intensity $B_\lambda(T)$ and therefore emits ε_λ times the blackbody radiant intensity. For a blackbody, absorption is a maximum and so is emission. Thus, we have

$$A_\lambda = \varepsilon_\lambda = 1 \tag{1.2.13}$$

for all wavelengths. A *gray body* is characterized by incomplete absorption and emission and may be described by

$$A_\lambda = \varepsilon_\lambda < 1. \tag{1.2.14}$$

Kirchhoff's law requires the condition of thermodynamic equilibrium, such that uniform temperature and isotropic radiation are achieved. Obviously, the radiation field of the earth's atmosphere as a whole is not isotropic and its temperatures are not uniform. However, in a localized volume below about 60–70 km, to a good approximation, it may be considered to be isotropic with a uniform temperature in which energy transitions are governed by molecular collisions. It is in the context of this local thermodynamic equilibrium (LTE) that Kirchhoff's law is applicable to the atmosphere. Departure from the LTE conditions will be discussed in Section 1.3.3.

1.3 Absorption Line Formation and Line Shape

1.3.1 Line Formation

Inspection of high-resolution spectroscopy reveals that the emission spectra of certain gases are composed of a large number of individual and characteristic spectral lines. In the previous section, we indicated that Planck successfully explained the nature of radiation from heated solid objects of which the cavity radiator formed the prototype. Such radiation generates continuous spectra, as opposed to line spectra. Planck's quantization ideas, properly extended, however, lead to an understanding of line spectra as well. In the following, we use the simplest hydrogen model to discuss emission and absorption line formation.

1.3.1.1 Bohr's Model

Investigation of the hydrogen spectrum led Bohr (1913) to postulate that the circular orbits of the electrons were quantized; that is, their angular momentum could have only integral multiples of a basic value. Bohr assumed that the hydrogen atom exists, like Planck's oscillators, in certain stationary states in which it does not radiate. Radiation occurs only when the atom makes a transition from one state with energy E_k to a state with lower energy E_j. Thus, we write

$$E_k - E_j = h\tilde{\nu}, \tag{1.3.1}$$

where $h\tilde{\nu}$ represents the quantum of energy carried away by the photon, which is emitted from the atom during the transition. The lowest energy state is called the *ground state* of the atom. When an electron of an atom absorbs energy due to a collision and jumps into a larger orbit, the atom is said to be in an *excited state*. Then, according to Eq. (1.3.1), a sudden transition will take place, and the atom emits a photon of energy and collapses to a lower energy state. This is illustrated in Fig. 1.8 for a hydrogen atom. Also shown in this figure is the absorption of a photon by a stationary hydrogen atom.

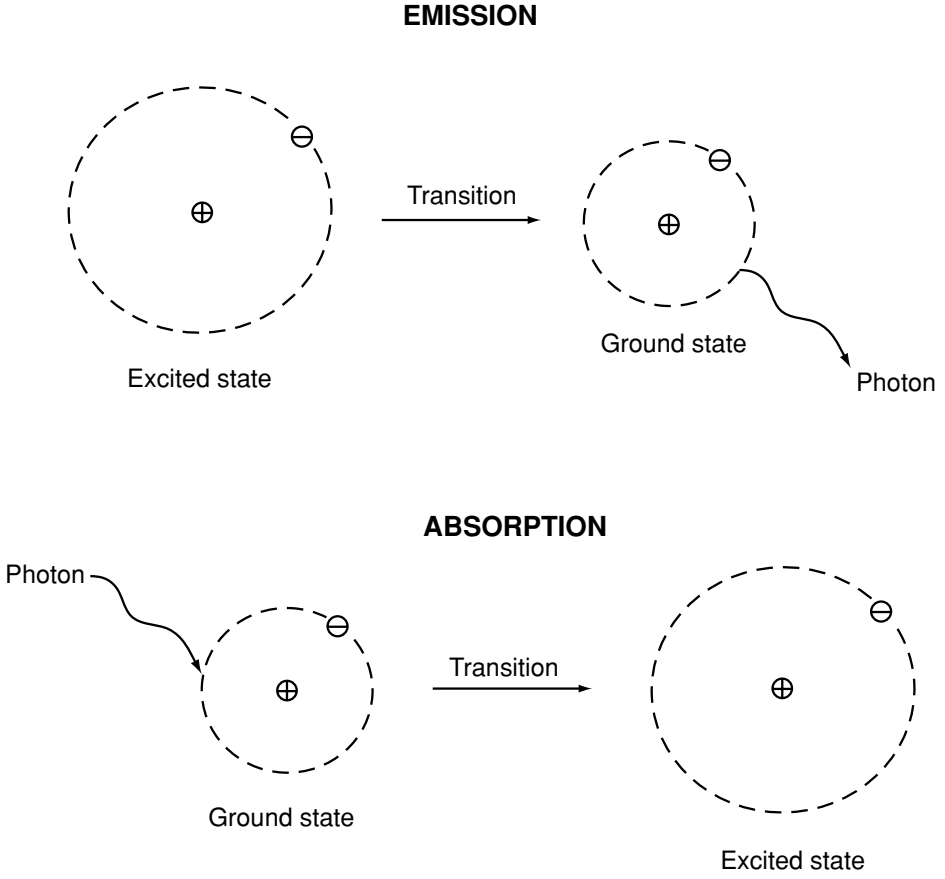

Figure 1.8 Illustration of emission and absorption for a hydrogen atom that is composed of one proton and one electron. The radius of the circular orbit r is given by $n^2 \times 0.53$ Å, where n is the quantum number, and $1\ \text{Å} = 10^{-8}$ cm.

Bohr further postulated that the angular momentum L can take on only discrete values by

$$L = n(h/2\pi), \quad n = 1, 2, 3 \ldots. \tag{1.3.2}$$

With this selection rule, Bohr showed from the equation of motion for an electron that the total energy state of the system is given by

$$E_n = -\frac{me^4}{8\varepsilon_0^2 h^2}\frac{1}{n^2} = -\frac{R_H hc}{n^2}, \quad n = 1, 2, 3 \ldots, \tag{1.3.3}$$

where m is the mass of the electron, e is the charge carried by the electron, ε_0 is the permittivity constant given by 8.85×10^{-12} coul/volt/m, with 1 volt = 1 joule/coul, and R_H is the *Rydberg constant* for hydrogen with a value of 1.097×10^5 cm^{-1}. It follows from Eq. (1.3.1) that the wavenumber of emission or absorption lines in the hydrogen spectrum is

$$\nu = R_H\left(\frac{1}{j^2} - \frac{1}{k^2}\right), \tag{1.3.4}$$

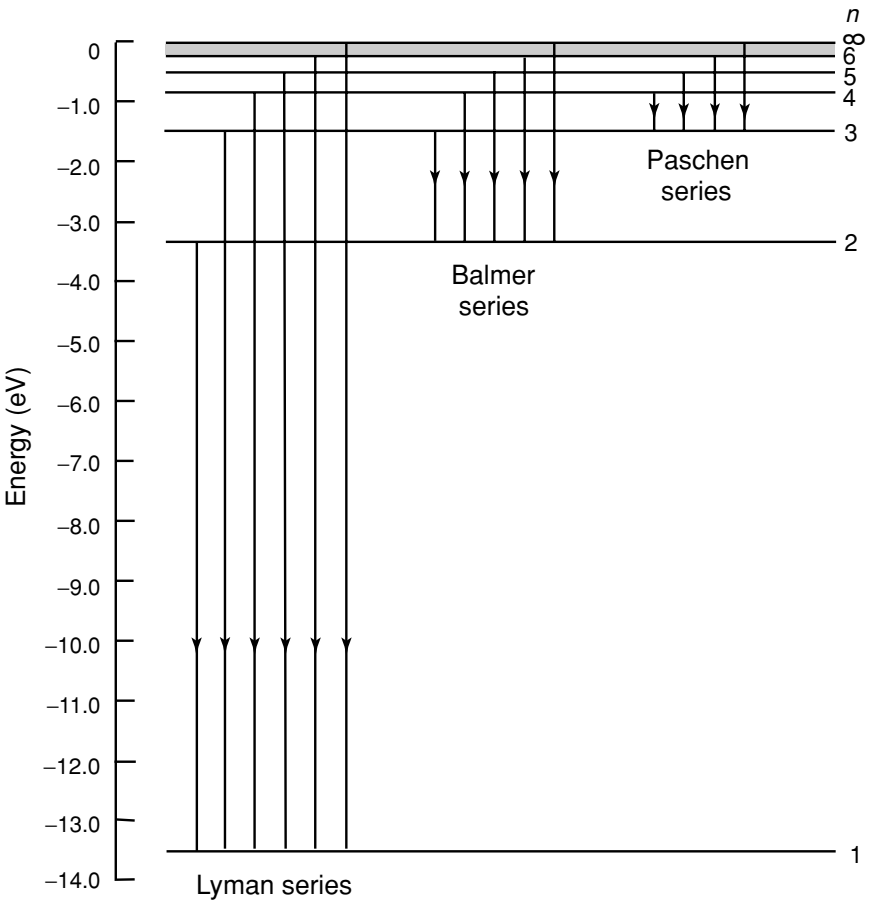

Figure 1.9 Energy level diagram for a hydrogen atom showing the quantum number n for each level and some of the transitions that appear in the spectrum. An infinite number of levels is crowded in between the levels marked $n = 6$ and $n = \infty$.

where j and k are integers defining, respectively, the lower and higher energy states. Figure 1.9 shows the energy diagram for hydrogen. In the field of spectroscopy, energy is usually given in units of electron volts (eV) or in units of wavenumber (cm^{-1}). An electron volt is the energy acquired by an electron accelerated through a potential difference of one volt, and is equivalent to 1.602×10^{-19} J. Exercise 1.11 requires the derivation of Eq. (1.3.3) based on the definitions of kinetic and potential energies of the system.

Each quantum jump between fixed energy levels results in the emission or absorption of a characteristic frequency or wavelength. These quanta appear in the spectrum as emission or absorption lines. For the simple hydrogen atom described previously the line spectrum is relatively simple, whereas the spectra of water vapor, carbon dioxide, and ozone molecules are considerably more complex.

1.3.1.2 Vibrational and Rotational Transitions

In the preceding discussion, we used the electronic transitions of the hydrogen atom to illustrate emission and absorption. It is now helpful to introduce the ways in which a molecule can store various energies. Any moving particle has kinetic

energy as a result of its motion in space. This is known as *translational energy*. The average translational kinetic energy of a single molecule in the x, y, and z directions is found to be equal to $KT/2$, where K is the Boltzmann constant and T is the absolute temperature. A molecule, composed of atoms, can rotate, or revolve, about an axis through its center of gravity and, therefore, has *rotational energy*. The atoms of the molecule are bounded by certain forces like springs such that the individual atoms can vibrate about their equilibrium positions relative to one another. The molecule, therefore, will also have *vibrational energy*. These three molecular energy types are based on a rather mechanical model of the molecule that ignores the detailed structure of the molecule in terms of nuclei and electrons. It is possible, however, for the energy of a molecule to change as a result of a change in the energy state of the electrons of which it is composed, as demonstrated by Bohr's model. Thus, the molecule has *electronic energy*. The last three energy types are quantized and take only discrete values. The absorption and emission of radiation takes place when the atoms or molecules undergo transitions from one energy state to another. In general, these transitions are governed by selection rules.

In radiative transitions, the molecule must couple with an electromagnetic field so that energy exchanges can take place. This coupling is generally provided by the electric dipole moment of the molecule. If the effective centers of the positive and negative charges of the molecule have nonzero separation, then the dipole moment exists. Radiatively active gases in the infrared, such as H_2O and O_3, have permanent electric dipole moments due to their asymmetrical charge distributions. Linear molecules such as N_2 and O_2, however, are inactive in the infrared because of their symmetrical charge distributions. However, they have weak magnetic dipole moments that allow radiative activities to take place in the ultraviolet and, to a lesser extent, in the visible region.

Rotational energy changes are relatively small, with a minimum on the order of $1\ \text{cm}^{-1}$ (see the conversion to energy in Exercise 1.12). For this reason, pure rotational lines occur in the microwave and far-infrared spectra. Many of the rotational energy levels above the lowest level are populated at terrestrial temperatures. Changes in vibrational energy are generally greater than $600\ \text{cm}^{-1}$, which is much larger than the minimum changes in rotational energy. Thus, vibrational transitions never occur alone but are coupled with simultaneous rotational transitions. This coupling gives rise to a group of lines known as the vibrational–rotational band in the intermediate infrared spectrum. An electronic transition typically involves a few electron volts ($\sim 10^4\ \text{cm}^{-1}$) of energy. Because a high-energy photon is required for the transition, absorption and emission usually occur in the ultraviolet or visible spectrum. Atoms can produce line spectra associated with electronic energy. Molecules, however, can have two additional types of energy, leading to complex band systems.

In Subsection 1.3.1.1, we discussed the physical meaning of stationary states for a hydrogen atom. Schrödinger (1926) first introduced the idea of stationary states corresponding to standing matter waves and used this idea as the foundation of *wave mechanics*. In quantum mechanics, to determine the energy states produced by vibrational and rotational transitions, a term referred to as the *Hamiltonian* operator, H,

was introduced as a convenient operator by replacing variables in the classical expression for the energy, E, of a system composed of the atomic nuclei and electrons that form a molecule. Schrödinger's equation can be written in terms of the first-order differential equation involving the wave function and the Hamiltonian operator, as shown in Appendix B. The Hamiltonian may be linearly separated into a time-dependent term and a time-independent term. The stationary states of the molecules can be deduced from the time-independent term, giving discrete eigenvalues (energy levels), E_n, and eigenfunctions, φ_n. Transitions between energy levels result in the absorption and emission of photons with frequency $\tilde{\nu}$ following Planck's relation. The time-dependent term may be treated as a perturbation from which the rate of change of the probability that a stationary state is occupied can be evaluated.

The Hamiltonian operator for the harmonic-oscillator rigid rotator is separable for vibrational and rotational motions so that energies may be added for a combined state. For the rotational states, the kinetic energy of a rigid rotating dipole is equal to one-half the product of angular momentum, L, and angular velocity, ω, i.e., $L\omega/2$, where $L = I\omega$ and I is the moment of inertia. From the solution of the time-independent Schrödinger equation, the quantum restrictions on angular momentum are given by

$$L = \frac{h}{2\pi}[J(J+1)]^{1/2}, \tag{1.3.5}$$

where J is the rotational quantum number (an integer). Thus, the quantized rotational energy can be written as

$$E_J = BhcJ(J+1), \tag{1.3.6}$$

where $B = h/8\pi^2 Ic$ is the rotational constant. This expression is valid for a rigid rotating dipole assuming spherical tops or linear molecules. For asymmetric tops, an additional term is required. The selection rule for radiation transition is governed by $\Delta J = \pm 1$, applicable to the harmonic-oscillator rigid-rotator model. From Planck's relation in Eq. (1.3.1), the spectral line location can be derived and is given by $\nu = 2BJ'$ (cm^{-1}), where J' can be any quantum number. Because of the selection rule, the separation in wavenumber of adjacent lines is simply $2B$ (cm^{-1}), as shown in Fig. 1.10a. As noted above, because of the small energy of a rotational transition, pure rotational spectra occur only in the far infrared and microwave regions.

For vibrational states, the quantized energy levels for a harmonic vibration are given by

$$E_\upsilon = h\tilde{\nu}_k(\upsilon_k + 1/2), \tag{1.3.7}$$

where υ_k is the vibrational quantum number (an integer) and subscript k denotes the normal modes. For triatomic molecules such as H_2O and O_3, there are three normal modes, referred to as *fundamentals*. For linear molecules such as CO_2 and NO_2, there are four fundamentals, but two orthogonal bending modes are degenerate and so only three fundamentals exist (see Fig. 3.3). The term *degenerate* is used to denote states with the same energy but with different sets of quantum numbers.

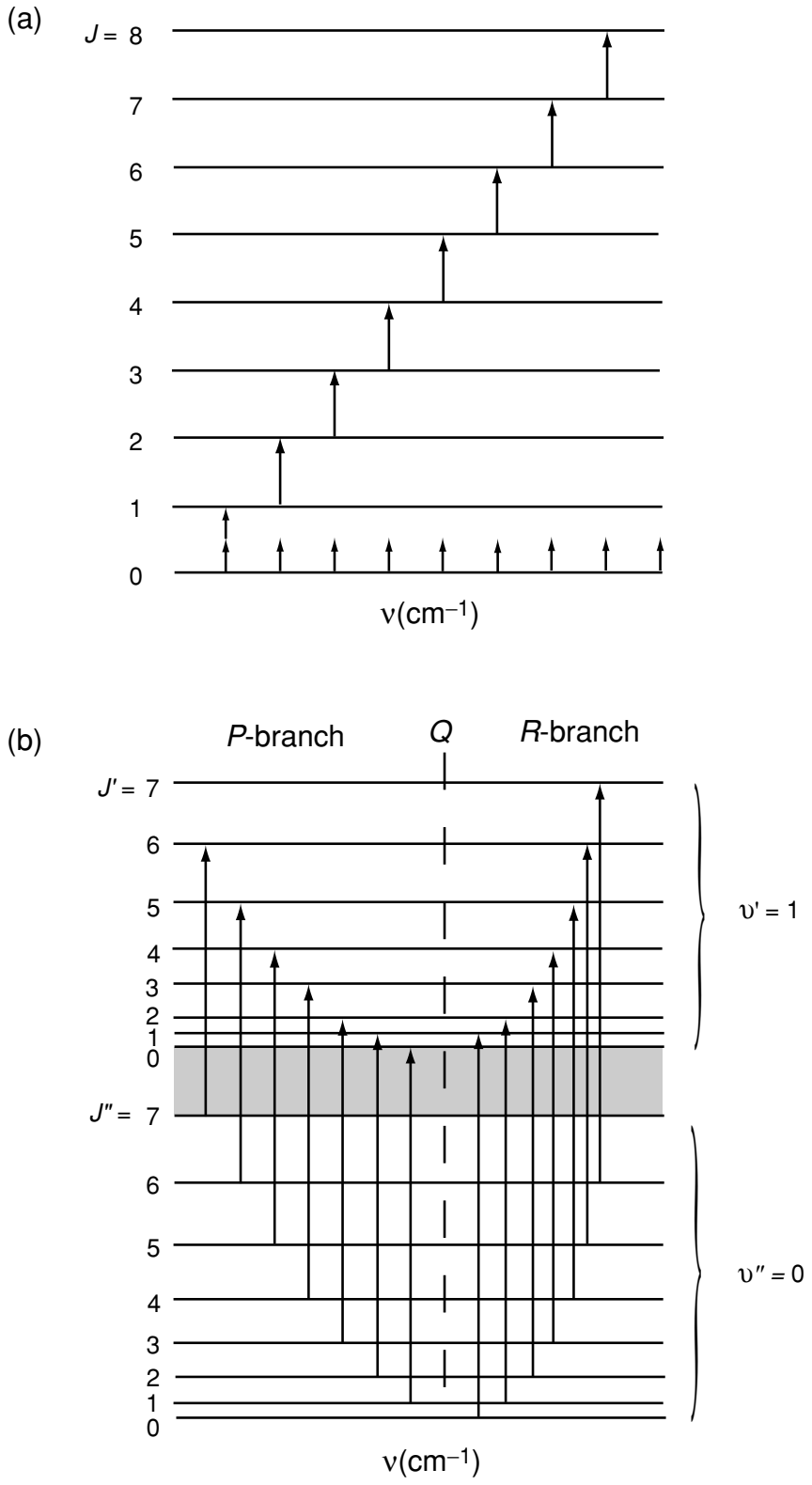

Figure 1.10 (a) Rotational transition following the selection rule $\Delta J = +1$ and equally spaced spectral lines in wavenumber. (b) Simultaneous vibrational and rotational transitions where $\Delta J = -1$ produces the P-branch and $\Delta J = +1$ generates the R-branch. $\Delta J = 0$ shows the Q-branch that overlaps with the vibrational wavenumber, but see text for discussion.

Molecular vibration produces an oscillating electric dipole moment that is sufficient for both vibrational and rotational transitions. Thus, both transitions occur simultaneously and the resulting energy level is the sum of the separate transition energies. Because the energy of the vibrational transition is much larger than that of the rotational transition as noted earlier, and since many rotational levels are active, the spectrum of the combined transitions is an array of rotational lines grouped around the vibrational wavenumber, as illustrated in Fig. 1.10b. From Eqs. (1.3.6) and (1.3.7), the sum of the rotational and vibrational energies is

$$E_{\upsilon,J} = BhcJ(J+1) + h\tilde{\nu}_k(\upsilon_k + 1/2). \tag{1.3.8}$$

In simple cases, the selection rule is $\Delta\upsilon_k = \pm 1$, except that $\Delta\upsilon_k = -1$ cannot be applied to $\upsilon_k = 0$. Consider the transitions $(\upsilon'_k, J') \leftarrow (\upsilon''_k, J'')$, and let $\upsilon''_k = 0$, the ground state, and $\upsilon'_k = 1$, the first excited state. J' and J'' denote the higher and lower rotational states, respectively, as shown in Fig. 1.10b. The selection rules in this case are $\Delta\upsilon_k = 1$ (fundamental) and $\Delta J = \pm 1$. Most of the molecules are in the ground state but are distributed over numerous levels of J''. Thus, any molecules advancing to the level υ' can go either to the next higher rotational level, for $\Delta J = +1$, or to the next lower level, for $\Delta J = -1$, with about equal probability. Using Planck's relation, we find that the spectral wavenumber of the line is given by

$$\nu = \nu_k \begin{cases} +2BJ',\ J' = 1, 2\ldots,\ \Delta J = +1, \\ -2B(J'+1),\ J' = 0, 1, \ldots,\ \Delta J = -1, \end{cases} \tag{1.3.9}$$

where J' is the rotational quantum number in the excited vibrational state υ'. Because many closely spaced rotational energy levels are involved, numerous transitions generate a band of rotational lines grouped on each side of the vibrational wavenumber, ν_k, with spacing of $2B$ cm^{-1}, as for a pure rotational spectrum. Several of the simultaneous transitions available to diatomic molecules and linear triatomic molecules (e.g., CO_2) in normal modes $k = 1(\upsilon_1)$ and $k = 3(\upsilon_3)$ fundamentals are shown schematically in Fig. 1.10b. The group with lower energy ($\Delta J = -1$) and hence the lower wavenumber portion of the band, is called the P-branch. The higher wavenumber part is referred to as the R-branch, corresponding to $\Delta J = +1$. The rotational level spacings in the υ' level are somewhat smaller than those in the υ'' level because of the increased moment of inertia in higher vibrational levels. The lengths of the arrows do not increase by a constant amount from the left to the right and the wavenumber spacing of the lines decreases slightly. The branches P and R are called *parallel branches* because the dipole moment oscillates parallel to the internuclear axis (see Fig. 3.3). For such vibrational modes the transition $\Delta J = 0$ is forbidden. In quantum mechanics, it is customary to refer to transitions as *forbidden* (or unfavorable) and *allowed*. For the vibrational mode $k = 2(\upsilon_2)$ of linear triatomic and the three modes of bent triatomic molecules (see Fig. 3.3), the change of dipole moment has a component perpendicular to an internuclear axis. The rotational selection rule is now $\Delta J = 0, \pm 1$, which produces a Q-branch that corresponds to $\Delta J = 0$, known as the *perpendicular branch*. This branch occurs at the vibrational frequency itself. In simple cases, it appears as a broad unresolved line. But if the moment of inertia differs

in the υ' and υ'' levels, the Q-branch may be seen as a group of very closely spaced lines.

The vibrational and rotational transitions discussed above are for the harmonic-oscillator rigid rotator in which the selection rules are given by $\Delta J = \pm 1$ and $\Delta\upsilon = \pm 1$. Because of the anharmonicity of the oscillator, the transition $\upsilon = 1 \leftarrow 0$ differs from the transition $\upsilon = 2 \leftarrow 1$. The upper-state band $2 \leftarrow 1$ does not have the same frequency as the ground-state band $1 \leftarrow 0$. Moreover, anharmonicity also changes the selection rules from those for a harmonic oscillator in which all integral changes of the quantum numbers are allowed. For example, $\Delta\upsilon = 2$ gives the first *overtone band* with twice the frequency of the normal (fundamental) mode. Simultaneous changes in two different vibrational quantum numbers give rise to *combination* and *difference bands* with frequencies that are the sum or difference of the normal-mode frequencies. They normally have smaller transition probabilities than fundamentals.

1.3.2 Line Broadening

Monochromatic emission is practically never observed. Energy levels during energy transitions are normally changed slightly due to both external influences on atoms and molecules, and the loss of energy in emission. As a consequence, radiation emitted during repeated energy transitions is nonmonochromatic, and spectral lines of finite widths are observed. The broadening of spectral lines is caused by: (1) the damping of oscillator vibrations resulting from the loss of energy in emission (the broadening of lines in this case is considered to be normal); (2) the perturbations due to reciprocal collisions between the absorbing molecules and between the absorbing and nonabsorbing molecules; and (3) the *Doppler effect* resulting from the difference in thermal velocities of atoms and molecules. The broadening of lines due to the loss of energy in emission (natural broadening) is practically negligible as compared to that caused by collisions and the Doppler effect. In the upper atmosphere, we find a combination of collision and Doppler broadenings, whereas in the lower atmosphere, below about 20 km, collision broadening prevails because of the pressure effect.

1.3.2.1 Pressure Broadening

The shape of spectral lines due to collisions, referred to as *pressure broadening,* is given by the *Lorentz profile* (Lorentz, 1906). It is expressed by the formula

$$k_\nu = \frac{S}{\pi}\frac{\alpha}{(\nu - \nu_0)^2 + \alpha^2} = Sf(\nu - \nu_0), \tag{1.3.10}$$

where k_ν denotes the absorption coefficient, ν_0 is the wavenumber of an ideal, monochromatic line, α is the half-width of the line at the half-maximum and is a function of pressure and to a lesser degree of the temperature, $f(\nu - \nu_0)$ represents the shape factor of a spectral line, and the line strength or line intensity S is defined by

$$\int_{-\infty}^{\infty} k_\nu d\nu = S. \tag{1.3.11}$$

In this case, we say the absorption coefficient is normalized. Figure 1.11 illustrates the Lorentz profile.

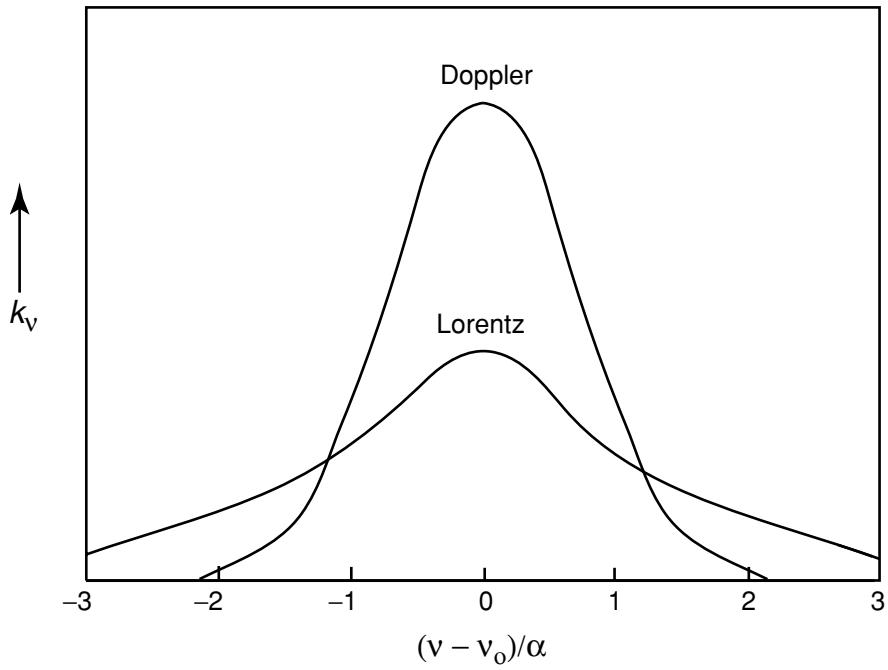

Figure 1.11 Demonstrative Lorentz and Doppler line shapes for the same intensities and line widths.

The Lorentz shape of absorption lines is fundamental to the theory of infrared radiative transfer in the atmosphere and thus, we should give a brief explanation of how the formula denoted in Eq. (1.3.10) is derived. An isolated molecule emits or absorbs an almost purely harmonic wave given by

$$f(t) = A \cos 2\pi \nu_0 ct, \tag{1.3.12a}$$

where c is the velocity of light and A is an arbitrary amplitude. During the period $-t/2$ to $t/2$, the distribution of amplitude $g(\nu)$ of the wave in the discrete wavenumber domain may be obtained from the Fourier cosine transform as follows:

$$\begin{aligned} g(\nu) &= \sqrt{\frac{2}{\pi}} \int_0^t (A \cos 2\pi \nu_0 ct') \cos 2\pi \nu ct' dt' \\ &= \frac{A}{(2\pi)^{3/2} c} \left[\frac{\sin \pi(\nu_0 + \nu)ct}{\nu_0 + \nu} + \frac{\sin \pi(\nu_0 - \nu)ct}{\nu_0 - \nu} \right]. \end{aligned} \tag{1.3.12b}$$

Generally, the widths of absorption lines are much smaller than ν_0, so that the first term in Eq. (1.3.12b) may be neglected when it is compared to the second.

The only deviation from purely harmonic behavior would be produced by the damping due to the loss of energy in emission. In the infrared, the spectroscopic effect of this damping is extremely small. However, if a radiating molecule collides with another molecule, it alters the radiating harmonic wave train due to the intermolecular forces, and the frequency of the emitting molecules would be temporarily shifted by an appreciable amount. Since the collision may be considered to be instantaneous, we may assume that the principal effect of the collision is to destroy the phase coherence of the emitted wave train. That is to say, after the collision the molecule starts emitting

at another phase and these new phases are now randomly distributed. From general statistical principles, the time between collisions is distributed according to Poisson's law that the probability a collision occurs between t and $t + dt$ is e^{-t/t_0}, where t_0 is the mean time between collisions. All the initial phases of the wave trains must be averaged. Thus, the absorption coefficient will be given by

$$k_\nu = A' \int_0^\infty [g(\nu)]^2 e^{-t/t_0}\, dt, \tag{1.3.13}$$

where $[g(\nu)]^2$ is the distribution of intensity, and A' is a certain constant. Further, by letting $1/t_0 = 2\pi\alpha c(\alpha \text{ in cm}^{-1})$ and using Eq. (1.3.11), we find that Eq. (1.3.13) becomes equivalent to Eq. (1.3.10). Here, $2\pi\alpha c$ is the number of collisions per molecule per unit time. [Exercise 1.14 requires the derivation of Eq. (1.3.10) from Eq. (1.3.13).] The Lorentz line shape also can be derived from the classical theory of absorption and dispersion as shown in Appendix D.

From the kinetic theory of gases, the dependence of the half-width α on pressure and temperature is given by

$$\alpha = \alpha_0(p/p_0)(T_0/T)^n, \tag{1.3.14}$$

where α_0 is the width at the standard pressure, p_0(1013mb), and temperature, T_0(273K). The index n ranges from $^1/_2$ to 1, depending on the type of molecule. When $n = {}^1/_2$, it is known as the classical value. Under the reference condition, α_0 ranges from about 0.01 to 0.1 cm^{-1} for most radiatively active gases in the earth's atmosphere and depends on the spectral line. For the CO_2 molecule, it is fairly constant with a value of about 0.07 cm^{-1} (see Section 4.2.1 for further discussion).

1.3.2.2 Doppler Broadening

Assuming that there is no collision broadening in a highly rarefied gas, a molecule in a given quantum state radiates at wavenumber ν_0. If this molecule has a velocity component in the line of sight (the line joining the molecule and the observer), and if $v \ll c$, the velocity of light, the wavenumber

$$\nu = \nu_0(1 \pm v/c). \tag{1.3.15}$$

Note that because of the conventional use of notation the wavenumber ν and the velocity v appear indistinguishable. Let the probability that the velocity component lies between v and $v + dv$ be $p(v)\,dv$. From the kinetic theory, if the translational states are in thermodynamic equilibrium, $p(v)$ is given by the Maxwell–Boltzmann distribution so that

$$p(v)\,dv = (m/2\pi KT)^{1/2} \exp(-mv^2/2KT)\,dv, \tag{1.3.16}$$

where m is the mass of the molecule, K is the Boltzmann constant, and T is the absolute temperature.

To obtain the Doppler distribution, we insert the expression of ν in Eq. (1.3.15) into Eq. (1.3.16), and perform normalization to an integrated line intensity S defined

in Eq. (1.3.11). After these operations, we find the absorption coefficient in the form

$$k_\nu = \frac{S}{\alpha_D\sqrt{\pi}} \exp\left[-\left(\frac{\nu-\nu_0}{\alpha_D}\right)^2\right], \tag{1.3.17}$$

where

$$\alpha_D = \nu_0(2KT/mc^2)^{1/2}, \tag{1.3.18}$$

is a measure of the Doppler width of the line. The half-width at the half-maximum is $\alpha_D\sqrt{\ln 2}$. The Doppler half-width is proportional to the square root of the temperature.

A graphical representation of the Doppler line shape is also shown in Fig. 1.11. Since the absorption coefficient of a Doppler line is dependent on $\exp[-(\nu-\nu_0)^2]$, it is more intense at the line center and much weaker in the wings than the Lorentz shape. This implies that when a line is fully absorbed at the center, any addition of absorption will occur in the wings and will be caused by collision effects rather than Doppler effects.

1.3.2.3 Voigt Profile

In the altitude region extending from about 20 to 50 km, effective line shapes are determined by both collision- and Doppler-broadening processes. We must add the Doppler shift component to the pressure-broadened lines at wavenumbers $\nu'-\nu_0$ in order to combine the two effects. The Doppler line redistributes the Lorentz line at wavenumber ν' to ν. The line shapes for pressure and Doppler broadening may then be expressed by $f(\nu'-\nu_0)$ and $f_D(\nu-\nu')$, respectively. To account for all possible thermal velocities, a convolution of the Lorentz and Doppler line shapes can be performed to obtain

$$\begin{aligned} f_\upsilon(\nu-\nu_0) &= \int_{-\infty}^{\infty} f(\nu'-\nu_0) f_D(\nu-\nu')\, d\nu' \\ &= \frac{1}{\pi^{3/2}}\frac{\alpha}{\alpha_D}\int_{-\infty}^{\infty} \frac{1}{(\nu'-\nu_0)^2+\alpha^2} \exp\left[\frac{-(\nu-\nu')^2}{\alpha_D^2}\right] d\nu'. \end{aligned} \tag{1.3.19a}$$

This line shape is referred to as the *Voigt profile*.

To simplify the representation of the Voigt profile, we let $t = (\nu-\nu')/\alpha_D$, $y = \alpha/\alpha_D$, and $x = (\nu-\nu_0)/\alpha_D$. Thus, we have

$$f_\upsilon(\nu-\nu_0) = \frac{1}{\alpha_D\sqrt{\pi}}\, K(x, y), \tag{1.3.19b}$$

where the Voigt function is defined by

$$K(x, y) = \frac{y}{\pi}\int_{-\infty}^{\infty} \frac{1}{y^2+(x-t)^2} e^{-t^2}\, dt. \tag{1.3.20}$$

Many attempts have been made to simplify the computation of the Voigt function. Closed-form approximations can be developed. The Voigt profile satisfies the requirement of normalization such that

$$\int_{-\infty}^{\infty} f_\upsilon(\nu - \nu_0) d(\nu - \nu_0) = 1. \tag{1.3.21}$$

Exercise 1.17 requires the derivation of Eq. (1.3.19b) and the proofs that in the limits of $\alpha \to 0$ and $\alpha_D \to 0$, the Voigt profile reduces to the Doppler and Lorentz shapes, respectively.

One final note is in order. The line strength of a specific molecule that undergoes a transition from an upper energy state i to a lower energy state j is proportional to the square of the transition probability defined by

$$\mathbf{R}_{ij} = \int \psi_i^* \mathbf{M} \psi_j \, dV, \tag{1.3.22}$$

where $\mathbf{M}$ is the matrix of the dipole moment related to the time-dependent Hamiltonian, V is the volume, $\psi_{i,j}$ are wave functions of the upper and lower energy states that can be determined from Schrödinger's equation, and ψ^* is the conjugate of ψ. The line strength for absorption also depends on the ratio of the population, n_j, of the lower energy state of the transition to the total population of the absorbing gas, n. At thermodynamic equilibrium, this ratio is defined by the Boltzmann factor in the form

$$n_j/n = g_j e^{-E_j/KT} \Big/ \sum_i g_i e^{-E_i/KT} \ , \tag{1.3.23}$$

where the integer g_j is called degenerate or statistical weight, which is the number of distinct states having energy E_j. The denominator on the right side of Eq. (1.3.23) is the *partition function,* which can be determined for both vibrational and rotational states.

1.3.3 Breakdown of Thermodynamic Equilibrium

In Section 1.2.4, we pointed out that in thermodynamic equilibrium, the source function is given by the Planck function, which depends only on temperature, frequency, and the velocity of light, and that within a small constant-temperature enclosure in which nothing changes, an element of matter absorbs and emits according to Planck's and Kirchhoff's laws. However, as was first pointed out by Einstein, emission is also affected by the incident radiation field, referred to as *induced emission*. In the following, we wish to address the extent to which the source function and absorption coefficient can be changed from their equilibrium values by the action of incident radiation. Since the discussion now involves departure from the equilibrium state, the thermodynamic arguments cannot be followed. We must now use a microscopic statistical model to understand the condition under which Kirchhoff's law cannot be applied.

Thermodynamic equilibrium can be defined in terms of Boltzmann's law for the distribution of molecules between two states. Consider a simple case where emission

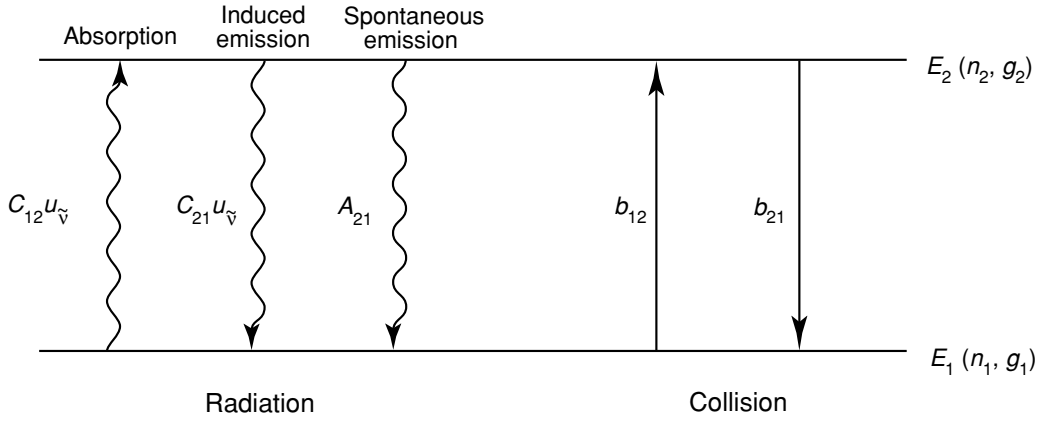

Figure 1.12 Radiative and collisional transitions connecting two energy states E_1 and E_2 where n_i are the numbers of molecules at the level E_i per unit volume; g_i are the statistical weights; b_{21} denotes the probability of transition by collisions per unit of time from the upper level E_2 to the lower level E_1 and b_{12} from E_1 to E_2; C_{12}, C_{21}, and A_{21} are the Einstein coefficients associated with emission and absorption; and $u_{\tilde{\nu}}$ denotes the radiant energy density.

(or absorption) occurs through transitions between the energy levels E_1 and E_2 of a two-level energy system, as shown in Fig. 1.12. Let n_1 and n_2 be the numbers of molecules at these levels per unit volume; and g_1 and g_2 denote the statistical weights, defined in Eq. (1.3.23). In accordance with Boltzmann's law, the distribution of molecules between two states is defined by

$$\frac{n_2}{n_1} = \frac{g_2}{g_1} \exp\left(-\frac{E_2 - E_1}{KT}\right) = \frac{g_2}{g_1} e^{-h\tilde{\nu}/KT}, \tag{1.3.24}$$

where $\tilde{\nu}$ is the emitting frequency from Planck's relation denoted in Eq. (1.3.1). Under complete equilibrium, Eq. (1.3.24) is obeyed for all energy states throughout the medium. It is known that collisions acting alone will bring about a Boltzmann distribution and consequently a Planck source function. However, in a collisionless medium, radiation can bring about almost any population of energy levels through absorption and induced emission involving a radiating molecule and a photon (C coefficients), as shown in Fig. 1.12. Radiative transitions can also take place spontaneously without the presence of a photon or a colliding molecule (A coefficients). This occurs from the upper level to the lower level. Including both collision and radiation processes, one can show from the balance of transitions between two energy levels that the state population ratio is given by

$$\frac{n_2}{n_1} = \frac{g_2}{g_1} \frac{\eta + u_{\tilde{\nu}}}{\eta \exp(h\tilde{\nu}/KT) + 8\pi h\tilde{\nu}^3/c^3 + u_{\tilde{\nu}}}, \tag{1.3.25}$$

where $u_{\tilde{\nu}}$ is the energy density and the coefficient that governs the relative importance of collision and radiation is defined by

$$\eta = \frac{b_{12}\,(\text{collision})}{C_{12}\,(\text{radiation})}. \tag{1.3.26}$$

Exercise 1.18 requires the derivation of Eq. (1.3.25). The population of energy levels and the resulting source functions will be governed by the conflict between radiative and collisional effects. The rate of collisional adjustment of state populations is determined by a relaxation time proportional to the pressure. Radiative adjustment is determined by the natural lifetime of the excited states with respect to radiative transitions and is dependent on specific molecules but independent of the state of the medium. When the collision events are much larger than the radiative transitions, then $\eta \gg 1$ and Eq. (1.3.25) reduces to Eq. (1.3.24). In this case, LTE should occur and Planck's law will be valid. On the other hand, if $\eta \ll 1$, then a different source function would be required. In the earth's atmosphere, pressure varies rapidly with height and since collisional processes are dependent on pressure, there will be a sharply defined relaxation level below which Planck's law (LTE) is valid for transitions between energy levels but above which a different source function will be required (non-LTE). This level occurs at about 60–70 km in the earth's atmosphere.

1.4 Introduction to Radiative Transfer

1.4.1 The Equation of Radiative Transfer

A pencil of radiation traversing a medium will be weakened by its interaction with matter. If the intensity of radiation I_λ becomes $I_\lambda + dI_\lambda$ after traversing a thickness ds in the direction of its propagation, then

$$dI_\lambda = -k_\lambda \rho I_\lambda \, ds, \tag{1.4.1}$$

where ρ is the density of the material, and k_λ denotes the mass extinction cross section (in units of area per mass) for radiation of wavelength λ. As discussed in Section 1.1.4, the mass extinction cross section is the sum of the mass absorption and scattering cross sections. Thus, the reduction in intensity is due to absorption by the material as well as to scattering by the material.

On the other hand, the radiation's intensity may be strengthened by emission from the material plus multiple scattering from all other directions into the pencil under consideration at the same wavelength (see Fig. 1.13). We define the source function coefficient j_λ such that the increase in intensity due to emission and multiple scattering is given by

$$dI_\lambda = j_\lambda \rho \, ds, \tag{1.4.2}$$

where the source function coefficient j_λ has the same physical meaning as the mass extinction cross section. Upon combining Eqs. (1.4.1) and (1.4.2), we obtain

$$dI_\lambda = -k_\lambda \rho I_\lambda \, ds + j_\lambda \rho \, ds. \tag{1.4.3}$$

Moreover, it is convenient to define the source function J_λ such that

$$J_\lambda \equiv j_\lambda / k_\lambda. \tag{1.4.4}$$

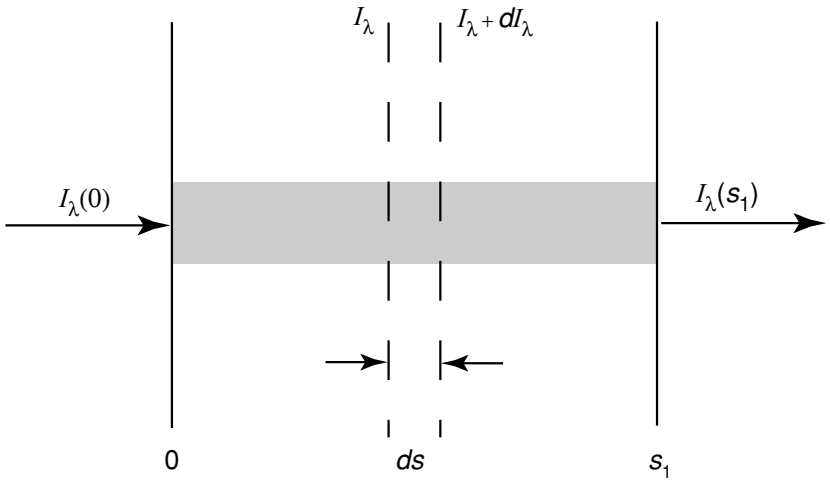

Figure 1.13 Depletion of the radiant intensity in traversing an extinction medium.

In this manner, the source function has units of radiant intensity. It follows that Eq. (1.4.3) may be rearranged to yield

$$\frac{dI_\lambda}{k_\lambda \rho\, ds} = -I_\lambda + J_\lambda. \tag{1.4.5}$$

This is the general radiative transfer equation without any coordinate system imposed, which is fundamental to the discussion of any radiative transfer process.

1.4.2 Beer–Bouguer–Lambert Law

Consider a direct light beam from the sun, which covers the wavelengths from about 0.2 to 5 μm. Emission contributions from the earth–atmosphere system can be generally neglected, as discussed in Section 1.2. Moreover, if the diffuse radiation produced by multiple scattering can be neglected, then Eq. (1.4.5) reduces to the following form:

$$\frac{dI_\lambda}{k_\lambda \rho\, ds} = -I_\lambda. \tag{1.4.6}$$

Let the incident intensity at $s = 0$ be $I_\lambda(0)$. Then the emergent intensity at a distance s away shown in Fig. 1.13 can be obtained by integrating Eq. (1.4.6) and is given by

$$I_\lambda(s_1) = I_\lambda(0) \exp\left(-\int_0^{s_1} k_\lambda \rho\, ds\right). \tag{1.4.7}$$

Assuming that the medium is homogeneous, so that k_λ is independent of the distance s, and defining the path length

$$u = \int_0^{s_1} \rho\, ds, \tag{1.4.8}$$

Eq. (1.4.7) can be expressed by

$$I_\lambda(s_1) = I_\lambda(0) e^{-k_\lambda u}. \tag{1.4.9}$$

This is known as Beer's law or Bouguer's law or Lambert's law, referred to here as the Beer–Bouguer–Lambert law, which states that the decrease in the radiant intensity traversing a homogeneous extinction medium is in accord with the simple exponential function whose argument is the product of the mass extinction cross section and the path length. Since this law involves no directional dependence, it is applicable not only to the intensity quantity but also to the flux density and the flux.

From Eq. (1.4.9), we can define the monochromatic transmissivity T_λ as follows:

$$T_\lambda = I_\lambda(s_1)/I_\lambda(0) = e^{-k_\lambda u}. \tag{1.4.10}$$

Moreover, for a nonscattering medium, the monochromatic absorptivity, representing the fractional part of the incident radiation that is absorbed by the medium, is given by

$$A_\lambda = 1 - T_\lambda = 1 - e^{-k_\lambda u}. \tag{1.4.11}$$

Equations (1.4.10) and (1.4.11) are normally expressed in the wavenumber domain in conjunction with the application of infrared radiation transfer. Finally, if there is a scattering contribution from the medium, certain portions of the incident radiation may reflect back to the incident direction. In this case, we may define the monochromatic reflectivity R_λ, which is the ratio of the reflected (backscattered) intensity to the incident intensity. On the basis of the conservation of energy, we must have

$$T_\lambda + A_\lambda + R_\lambda = 1 \tag{1.4.12}$$

for the transfer of radiation through a scattering and absorbing medium.

1.4.3 Schwarzschild's Equation and Its Solution

Consider a nonscattering medium that is in local thermodynamic equilibrium. A beam of intensity I_λ passing through it will undergo the absorption and emission processes simultaneously. This is the case for the transfer of thermal infrared radiation emitted from the earth and the atmosphere. The source function, as defined in Eq. (1.4.4), is given by the Planck function and can be expressed by

$$J_\lambda = B_\lambda(T). \tag{1.4.13}$$

Hence, the equation of radiative transfer can now be written as

$$\frac{dI_\lambda}{k_\lambda \rho\, ds} = -I_\lambda + B_\lambda(T), \tag{1.4.14}$$

where k_λ is now the absorption coefficient. The first term in the right-hand side of Eq. (1.4.14) denotes the reduction of the radiant intensity due to absorption, whereas the second term represents the increase in the radiant intensity arising from blackbody emission of the material. To seek a solution for Schwarzschild's equation, we define the monochromatic optical thickness of the medium between points s and s_1 as shown

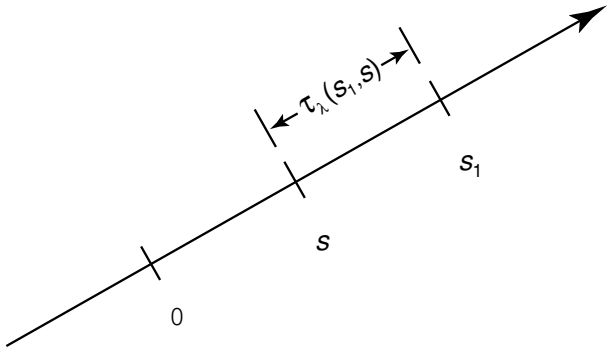

Figure 1.14 Configuration of the optical thickness τ_λ defined in Eq. (1.4.15).

in Fig. 1.14 in the form

$$\tau_\lambda(s_1, s) = \int_s^{s_1} k_\lambda \rho \, ds'. \tag{1.4.15}$$

By noting that

$$d\tau_\lambda(s_1, s) = -k_\lambda \rho \, ds, \tag{1.4.16}$$

Eq. (1.4.14) becomes

$$-\frac{dI_\lambda(s)}{d\tau_\lambda(s_1, s)} = -I_\lambda(s) + B_\lambda[T(s)]. \tag{1.4.17}$$

Upon multiplying Eq. (1.4.17) by a factor $e^{-\tau_\lambda(s_1,s)}$, and integrating the thickness ds from 0 to s_1, we obtain

$$-\int_0^{s_1} d[I_\lambda(s)e^{-\tau_\lambda(s_1,s)}] = \int_0^{s_1} B_\lambda[T(s)]e^{-\tau_\lambda(s_1,s)} d\tau_\lambda(s_1, s). \tag{1.4.18}$$

Consequently, we have

$$I_\lambda(s_1) = I_\lambda(0)e^{-\tau_\lambda(s_1,0)} + \int_0^{s_1} B_\lambda[T(s)]e^{-\tau_\lambda(s_1,s)} k_\lambda \rho \, ds. \tag{1.4.19}$$

The first term in Eq. (1.4.19) is essentially equivalent to Eq. (1.4.7), representing the absorption attentuation of the radiant intensity by the medium. The second term denotes the emission contribution from the medium along the path from 0 to s_1. If the temperature and density of the medium and the associated absorption coefficient along the path of the beam are known, Eq. (1.4.19) can be integrated numerically to yield the intensity at the point s_1. Applications of Eq. (1.4.19) to infrared radiative transfer and to the remote sounding of atmospheric temperature profiles and compositions from orbiting meteorological satellites will be discussed in Chapters 4 and 7, respectively.

In the discussion of the absorption and emission lines in the spectra of sun and stars, Schwarzschild (1914) presented Eq. (1.4.14) within the context of Kirchhoff's law and derived an integral solution for the condition without scattering. It is thus referred to as Schwarzschild's equation.

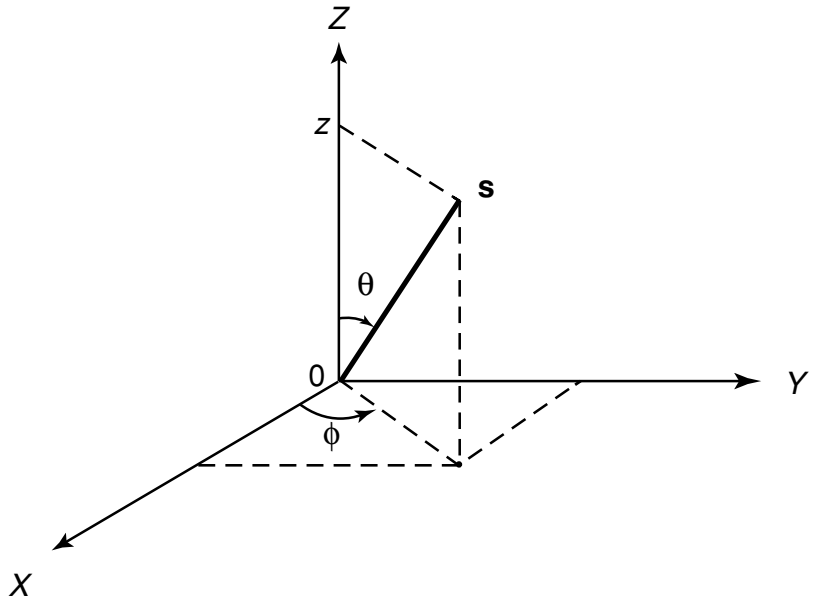

Figure 1.15 Geometry for plane-parallel atmospheres where θ and ϕ denote the zenith and azimuthal angles, respectively, and **s** represents the position vector.

1.4.4 The Equation of Radiative Transfer for Plane-Parallel Atmospheres

For many atmospheric radiative transfer applications, it is physically appropriate to consider that the atmosphere in localized portions is plane-parallel such that variations in the intensity and atmospheric parameters (temperature and gaseous profiles) are permitted only in the vertical direction (i.e., height and pressure). In this case, it is convenient to measure linear distances normal to the plane of stratification (see Fig. 1.15). If z denotes this distance, then the general equation of radiative transfer defined in Eq. (1.4.5) becomes

$$\cos\theta \frac{dI(z;\theta,\phi)}{k\rho\, dz} = -I(z;\theta,\phi) + J(z;\theta,\phi), \tag{1.4.20}$$

where θ denotes the inclination to the upward normal, and ϕ the azimuthal angle in reference to the x axis. Here, we have omitted the subscript λ on various radiative quantities.

Introducing the normal optical thickness (or depth)

$$\tau = \int_z^\infty k\rho\, dz' \tag{1.4.21}$$

measured downward from the outer boundary, we have

$$\mu \frac{dI(\tau;\mu,\phi)}{d\tau} = I(\tau;\mu,\phi) - J(\tau;\mu,\phi), \tag{1.4.22}$$

where $\mu = \cos\theta$. This is the basic equation for the problem of multiple scattering in plane-parallel atmospheres.

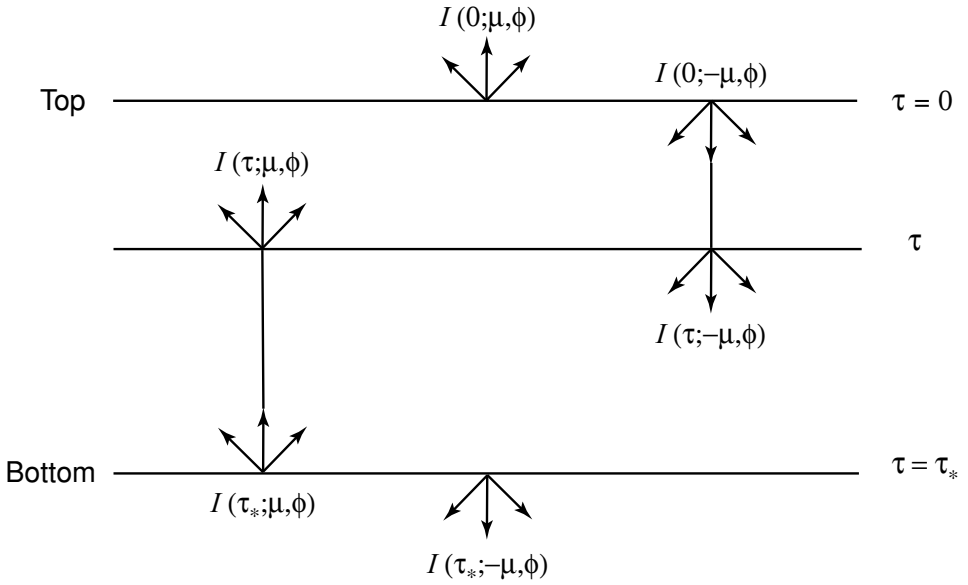

Figure 1.16 Upward (μ) and downward ($-\mu$) intensities at a given level τ and at top ($\tau = 0$) and bottom ($\tau = \tau_*$) levels in a finite, plane-parallel atmosphere.

Following the same procedure as that described in Section 1.4.3, Eq. (1.4.22) can be solved to give the upward and downward intensities for a finite atmosphere that is bounded on two sides at $\tau = 0$ and $\tau = \tau_*$ as illustrated in Fig. 1.16. To obtain the upward intensity ($\mu > 0$) at level τ, we multiply Eq. (1.4.22) by a factor $e^{-\tau/\mu}$ and perform integration from τ to $\tau = \tau_*$. This leads to

$$I(\tau;\mu,\phi) = I(\tau_*;\mu,\phi)e^{-(\tau_*-\tau)/\mu} + \int_\tau^{\tau_*} J(\tau';\mu,\phi)e^{-(\tau'-\tau)/\mu}\frac{d\tau'}{\mu}\,(1 \geq \mu > 0). \tag{1.4.23}$$

To derive the downward intensity ($\mu < 0$) at level τ, a factor $e^{\tau/\mu}$ is used and μ is replaced by $-\mu$. After carrying out integration from $\tau = 0$ to τ, we obtain

$$I(\tau;-\mu,\phi) = I(0;-\mu,\phi)e^{-\tau/\mu} + \int_0^{\tau} J(\tau';-\mu,\phi)e^{-(\tau-\tau')/\mu}\frac{d\tau'}{\mu}\,(1 \geq \mu > 0). \tag{1.4.24}$$

In Eqs. (1.4.23) and (1.4.24), $I(\tau_*;\mu,\phi)$ and $I(0;-\mu,\phi)$ represent the inward source intensities at the bottom and top surfaces, respectively, as shown in Fig. 1.16.

For applications to planetary atmospheres, it is desirable to measure the emergent outward intensities at the top and bottom of the atmosphere in conjunction with the remote sensing of atmospheric compositions and radiation balance studies. Upon setting $\tau = 0$ in Eq. (1.4.23), we have

$$I(0;\mu,\phi) = I(\tau_*;\mu,\phi)e^{-\tau_*/\mu} + \int_0^{\tau_*} J(\tau';\mu,\phi)e^{-\tau'/\mu}\frac{d\tau'}{\mu}, \tag{1.4.25}$$

where the first and second terms represent, respectively, the bottom surface contribution (attenuated to the top) and the internal atmospheric contribution. On the other

hand, if we set $\tau = \tau_*$ in Eq. (1.4.24), we obtain

$$I(\tau_*; -\mu, \phi) = I(0; -\mu, \phi)e^{-\tau_*/\mu} + \int_0^{\tau_*} J(\tau'; -\mu, \phi)e^{-(\tau_* - \tau')/\mu} \frac{d\tau'}{\mu}, \quad (1.4.26)$$

where, again, the first and second terms represent the top surface contribution (attenuated to the bottom) and the internal atmospheric contribution, respectively. Detailed applications of the preceding equations associated with infrared radiation transfer and multiple scattering will be discussed in Chapters 4 and 6.

1.4.5 Radiative Transfer Equations for Three-Dimensional Inhomogeneous Media

In several atmospheric conditions, the plane-parallel assumption may not be valid. These include the transfer of radiation in the atmosphere where spherical geometry must be accounted for, and in clouds with finite dimension and/or inhomogeneity in the horizontal direction. The latter has been a subject of contemporary research and development in conjunction with studies of clouds in climate and remote sensing. Although this topic will be further elaborated upon in Chapter 6, here we provide some introductory notes consistent with the preceding presentation. We begin with the general equation of radiative transfer discussed in Section 1.4.1. Letting the extinction coefficient be $\beta_e = k_\lambda \rho$ and omitting the subscript λ for simplicity, we write

$$-\frac{dI}{\beta_e \, ds} = I - J. \quad (1.4.27)$$

The differential operator can be defined in time and space as follows:

$$\frac{d}{ds} = \frac{1}{c}\frac{\partial}{\partial t} + \mathbf{\Omega} \cdot \boldsymbol{\nabla}, \quad (1.4.28)$$

where c is the velocity of light, $\mathbf{\Omega}$ is a unit vector specifying the direction of scattering through a position vector $\mathbf{s}$, and t is time. Under the condition that radiation is independent of time (steady state), such as the illumination from the sun, Eq. (1.4.27) can be expressed by

$$-\frac{1}{\beta_e(\mathbf{s})}(\mathbf{\Omega} \cdot \boldsymbol{\nabla})I(\mathbf{s}, \mathbf{\Omega}) = I(\mathbf{s}, \mathbf{\Omega}) - J(\mathbf{s}, \mathbf{\Omega}), \quad (1.4.29a)$$

where the source function, J, can be produced by the single scattering of the direct solar beam, multiple scattering of the diffuse intensity, and emission of the medium.

In Cartesian coordinates (x, y, z), we have

$$\mathbf{\Omega} \cdot \boldsymbol{\nabla} = \Omega_x \frac{\partial}{\partial x} + \Omega_y \frac{\partial}{\partial y} + \Omega_z \frac{\partial}{\partial z}, \quad (1.4.29b)$$

where the directional cosines are given by

$$\Omega_x = \frac{\partial x}{\partial s} = \sin\theta \, \cos\phi = (1 - \mu^2)^{1/2} \cos \, \phi, \quad (1.4.30a)$$

$$\Omega_y = \frac{\partial y}{\partial s} = \sin\theta \, \sin\phi = (1-\mu^2)^{1/2} \sin \phi, \tag{1.4.30b}$$

$$\Omega_z = \frac{\partial z}{\partial s} = \cos\theta = \mu, \tag{1.4.30c}$$

where θ and ϕ are the zenith and azimuthal angles defined previously, and $|\mathbf{s}| = s = (x^2 + y^2 + z^2)^{1/2}$. In general, analytic solutions for Eq. (1.4.29a) do not exist and it must be solved numerically. In cases where the medium is homogeneous with respect to its single-scattering properties including the extinction coefficient, Eq. (1.4.29a) reduces to a first-order partial differential equation from which simplified solutions can be derived. Interested readers should refer to Chapter 6 for further details.

Exercises

1.1 What is the meaning of isotropic radiation? Show that for isotropic radiation, the monochromatic flux density is $F_\lambda = \pi I_\lambda$.

1.2 A meteorological satellite circles the earth at a height h above the earth's surface. Let the radius of the earth be a_e and show that the solid angle under which the earth is seen by the satellite sensor is $2\pi[1 - (2a_e h + h^2)^{1/2}/(a_e + h)]$.

1.3 Express the Planck function in the wavelength and wavenumber domains based on the Planck function in the frequency domain.

1.4 From Eq. (1.2.10), show that Eq. (1.2.11) is true.

1.5 Show that the maximum intensity of the Planck function is proportional to the fifth power of the temperature.

1.6 An infrared scanning radiometer aboard a meteorological satellite measures the outgoing radiation emitted from the earth's surface in the 10 μm window region. Assuming that the effect of the atmosphere between the satellite and the surface can be neglected, what would be the temperature of the surface if the observed radiance at 10 μm is 9.8 W m^{-2} μm^{-1} sr^{-1}?

1.7 A black land surface with a temperature of 15°C emits radiation at all frequencies. What would be the emitted radiances at 0.7 μm, 1000 cm^{-1}, and 31.4 GHz? Use appropriate Planck functions in the calculations.

1.8 Assuming the average normal body temperature is 98°F, what would be the emittance of the body? If it is not a blackbody but absorbs only 90% of the incoming radiation averaged over all wavelengths, what would be the emittance in this case? Also, at which wavelength does the body emit the maximum energy?

1.9 (a) The photosphere of the sun has a temperature of about 5800 K. Assuming it is a blackbody, compute the percentage of its emitting intensity at wavelengths longer than 5 μm. (b) The earth–atmosphere system has an equilibrium temperature of about 255 K. Assume it can be considered a blackbody and compute the percentage of its emitting intensity at wavelengths shorter than 5 μm.

1.10 Show that when $\lambda \to \infty$, the Planck intensity is directly proportional to the temperature, referred to as the Rayleigh–Jeans distribution. When $\lambda \to 0$, derive the expression referred to as the Wien distribution. Plot the Planck intensity for the temperatures of the sun and the earth–atmosphere system and compare these two approximations with the exact values.

1.11 (a) From Newton's second law of motion and Coulomb's law, find the kinetic energy of an electron in a hydrogen atom moving with a velocity v in a circular orbit of radius r centered on its nucleus. Express r in terms of the quantum number n using the selection rule for the angular momentum mvr. Then find the potential energy of the proton–electron system. By combining the kinetic and potential energy, derive Eq. (1.3.3). (b) Considering only the transitions between the ground state ($n = 1$) and the excited states and letting the highest quantum number be 6, compute the wavelengths of hydrogen emission lines.

1.12 In spectroscopy, the wavenumber ν in cm^{-1} is not only used to specify a spectral location, but also as a measure of energy itself. From the energy equation, compute 1 cm^{-1} of energy of terms of 1 joule per molecule.

1.13 (a) Derive Eq. (1.3.9) from Eq. (1.3.8). (b) For the Q-branch, show that the line spacing is proportional to the difference of the rotational constants in the ground and excited states.

1.14 Derive Eq. (1.3.10) from Eq. (1.3.13).

1.15 Prove that the line intensity $S = \int_{-\infty}^{\infty} k_\nu \, d\nu$ for Lorentz, Doppler, and Voigt absorption lines.

1.16 Calculate and plot the shape factor of the Lorentz and Doppler profiles for ozone whose half-width is assumed to be 0.1 cm^{-1} in the wavenumber domain at the standard temperature and pressure.

1.17 Derive Eq. (1.3.19b) from Eq. (1.3.19a). In the limits of $\alpha \to 0$ and $\alpha_D \to 0$, show that the Voigt profile reduces to the Doppler and Lorentz shapes, respectively.

1.18 (a) From Eq. (1.3.24) for collision, derive an expression for b_{12}/b_{21} from n_2/n_1. (b) For radiation, show that $C_{21}/C_{12} = g_1/g_2$ and $A_{21}/C_{12} = g_1/g_2 \cdot 8\pi h\tilde{\nu}^3/c^3$, where $u_{\tilde{\nu}}$ is the energy density defined in Appendix A. (c) Then, based on the balance of transitions between two energy levels (Fig. 1.12), show that the state population ratio for the general case is given by Eq. (1.3.25).

1.19 A He–Ne laser beam at 0.6328 μm with an output power of 5 mW (10^{-3} W) is passing through an artificial cloud layer 10 m in thickness and is directed at 30° from the normal to the layer. Neglecting the effect of multiple scattering, calculate the extinction coefficients (per length) if the measured powers are 1.57576 and 0.01554 mW. Also calculate the normal optical depths in these cases.

1.20 The contrast of an object against its surroundings is defined by

$$C \equiv (B - B_0)/B_0,$$